Advanced 1
Introduction
Applications and Examples of Micro-Nano Mechatronics

Prof. T. Fukuda and Prof. F. Arai

Dept. of Micro/Nano Systems Engineering

Nagoya University

Technologies for Micro-Nano echatronics

Micro-Nano fabrication

- MEMS
- NEMS
- Machining
- Assembly
- Optics/Imaging

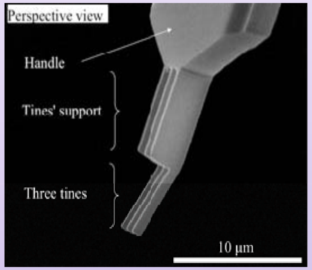

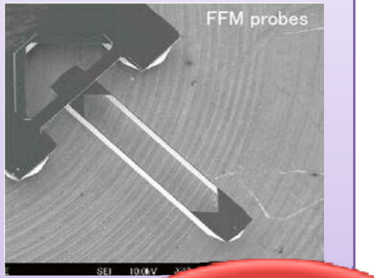

Micro-Nano Mechatronics

Robot technology

- Sensors
- Actuators
- Control theory
- Dynamics

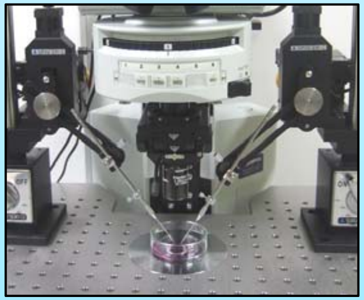

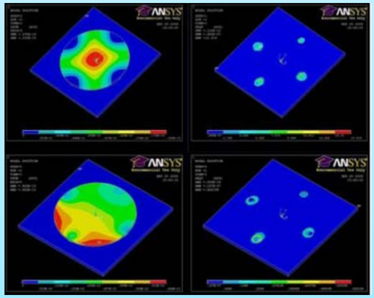

Micro-Nano Materials

- Tribology
- Energy
- Synthesis

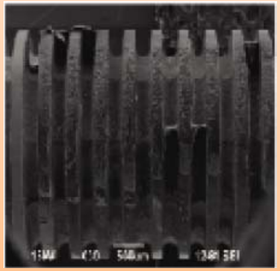

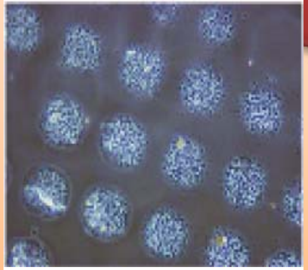

Application Fields of Micro-Nano Mechatronics

Medical field

- Surgical devices
- Endoscopic devices
- Training
- Diagnosis devices
- Implantation devices
- Welfare

Industrial field

- Micro size sensors
- Hi-sensitive sensors
- Integrated packaging
- Wireless technology
- Cost reduction
- New energy

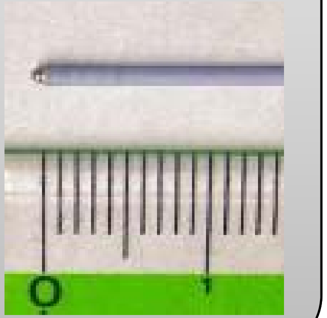

Bio field

- Single cell sensing
- Drug delivery
- Genome analysis
- Biofuel
- Cell assembly
- Tissue engineering

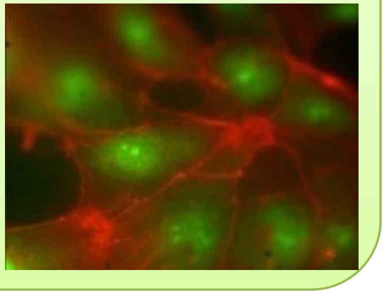

Fundamental research field

- New technology establishing
- New material
- New observation

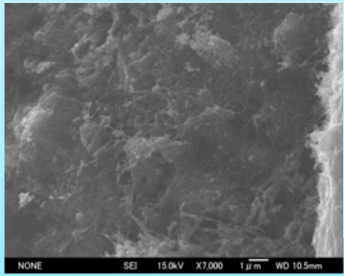

Application Examples

- Medical Field -

Background

ESD (Endoscopic Sub-mucosal Dissection)

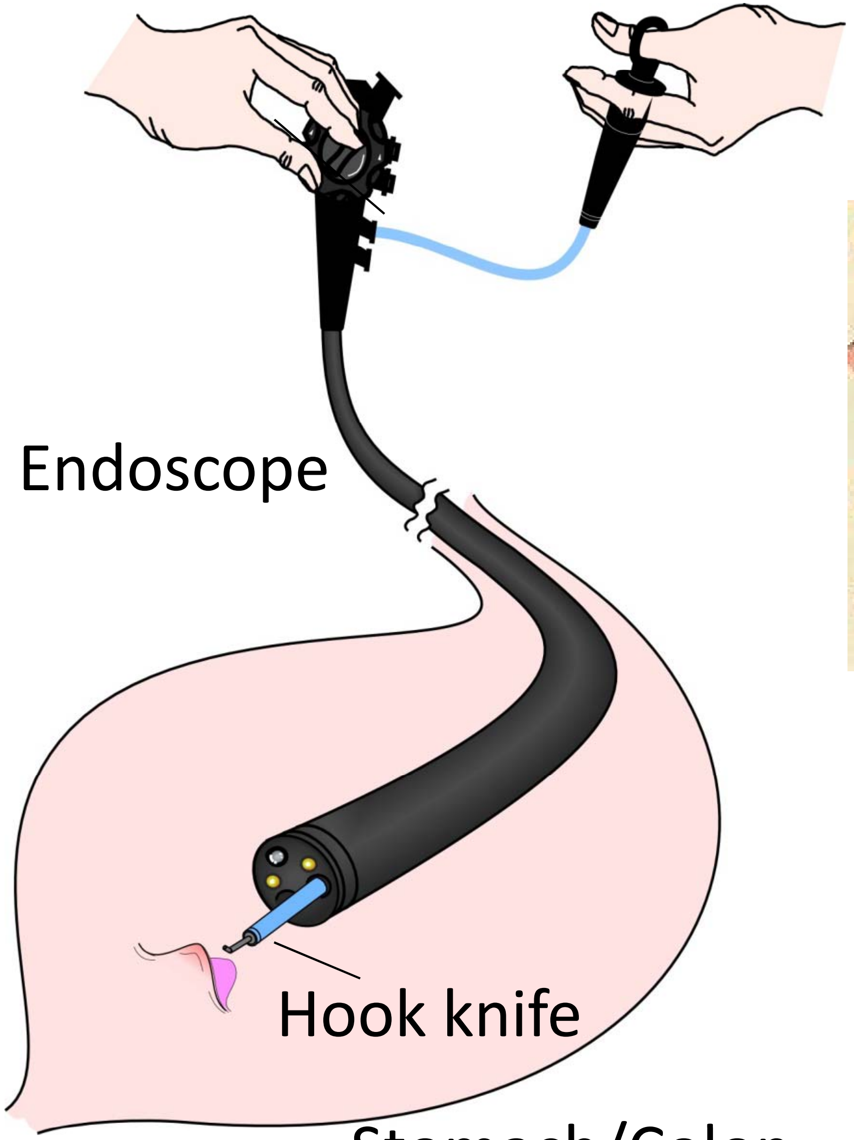

Endoscope

Hook knife

Stomach/Colon

Excision procedure

Cancer

Marking

Cutting

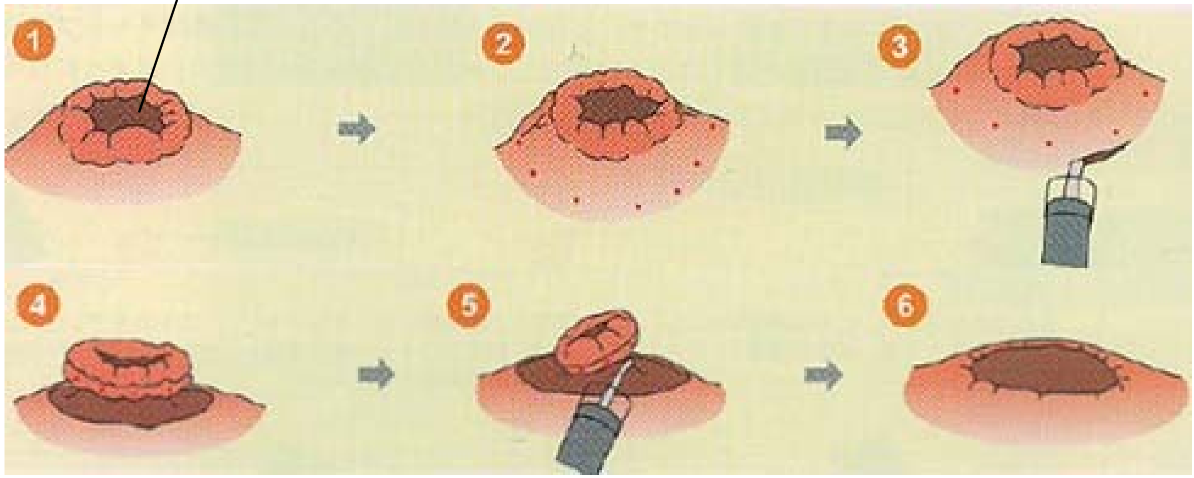

Exfoliating

Advantages
- Minimally invasive procedure
- Quick recovery

Problems
- Time-consuming
- Skill-dependent

Rerated Works

Clinical Field

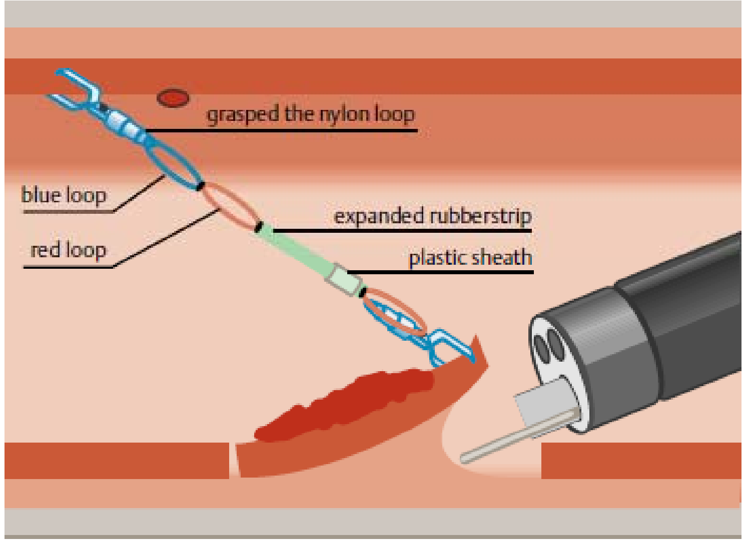

S−O clip, Sakamoto et al. (2008)

Reserach Field

Ikuta et al. (2000)
5DOF 3.0mm

Fujie et al. (2005)
3DOF 2.4mm

Olympus Medical
EndoSAMURAI

Nokata et al. (2010)
3DOF 1.4mm

(Year)

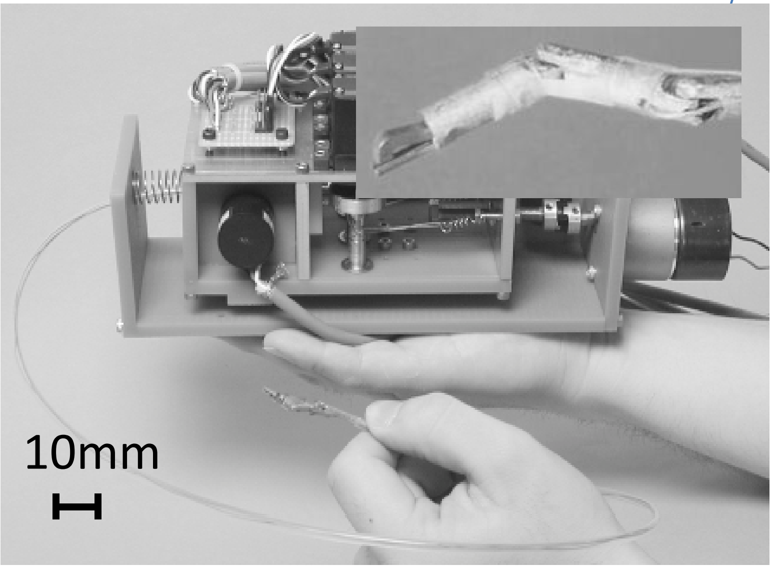

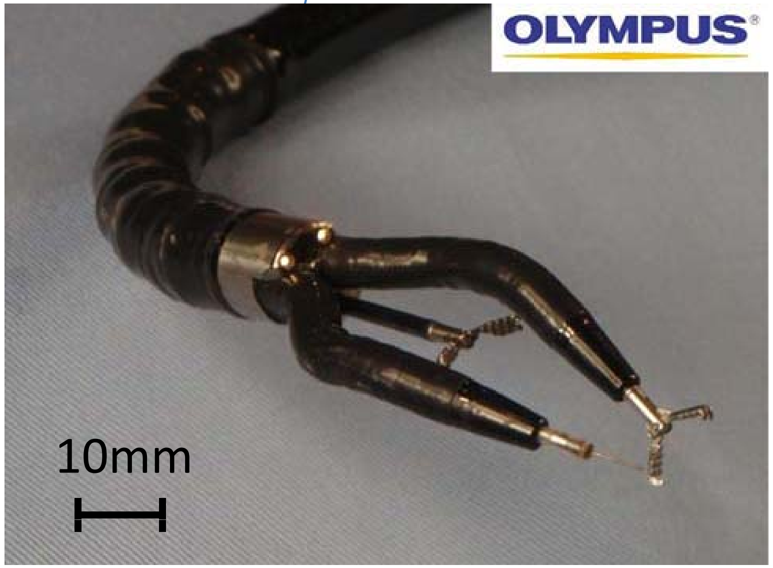

Decoupling Wire Driven Microarm

Design of 2DOF microarm (less than 3mm)

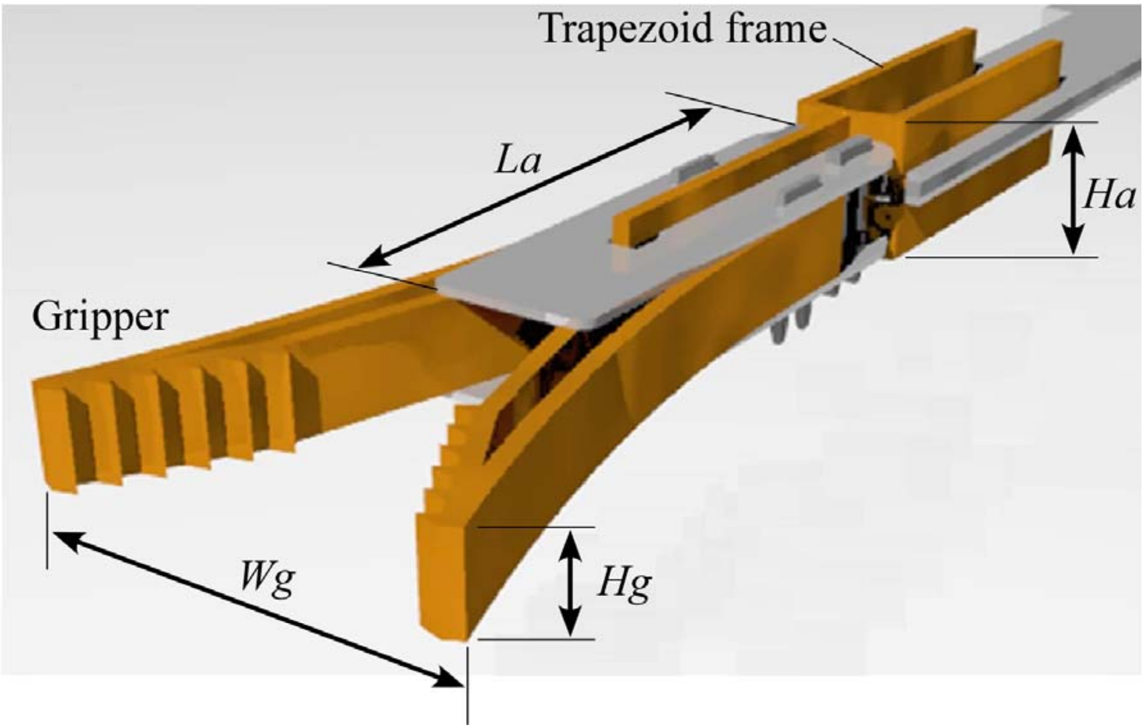

Channel
(ϕ3 mm)

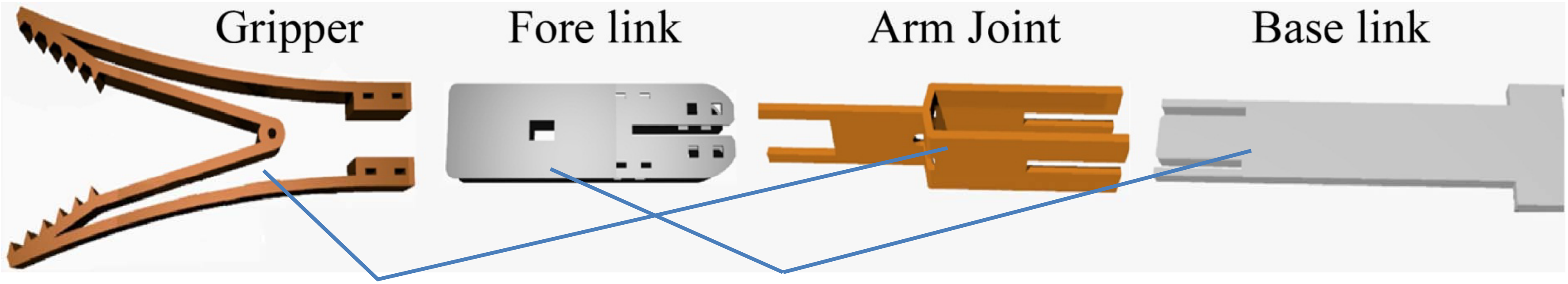

Wire-electric discharge   Photolithography

Ref.) Kawahara et al., Biorob, 2010

Wire Decoupling Design

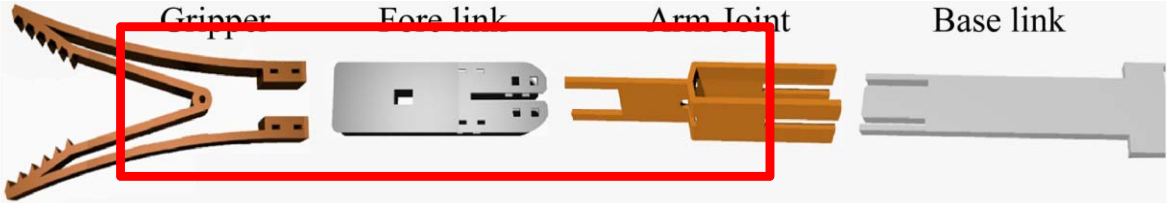

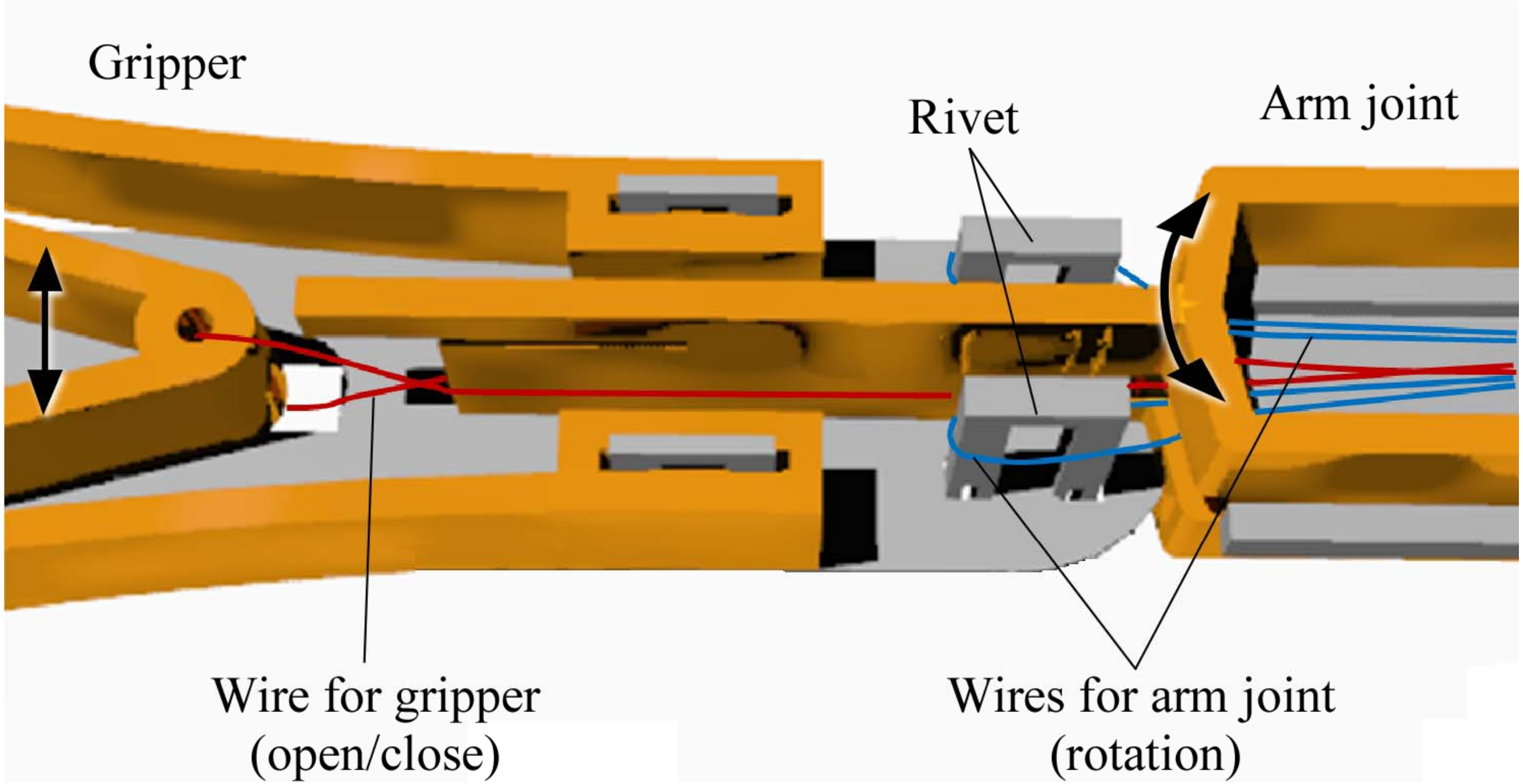

To achieve the wire decoupling, this wire for gripper is precisely passed through the center position of the arm joint.

Joint Design

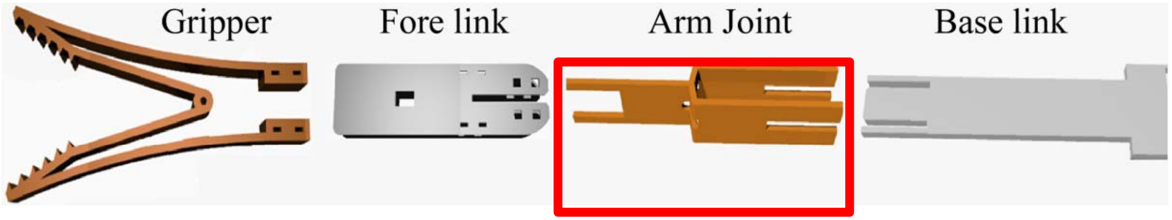

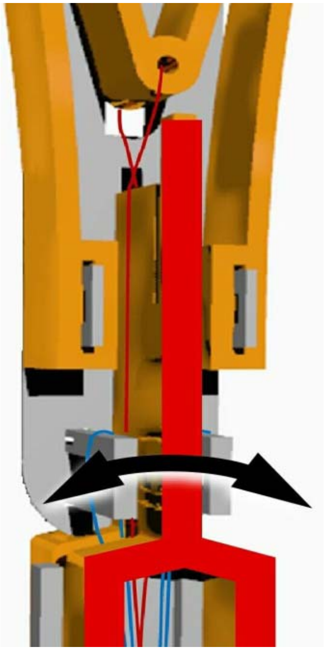

Trapezoid frame

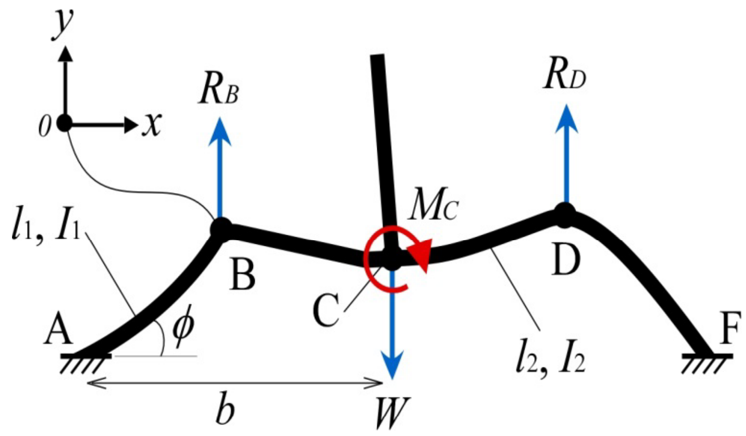

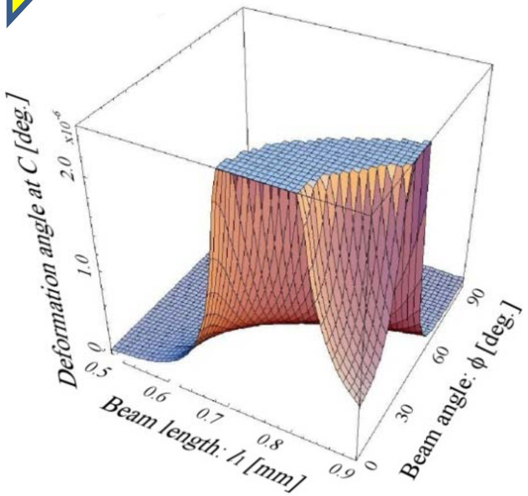

l_1=0.67 mm
l_2=0.00 mm
ϕ=12.0 deg.

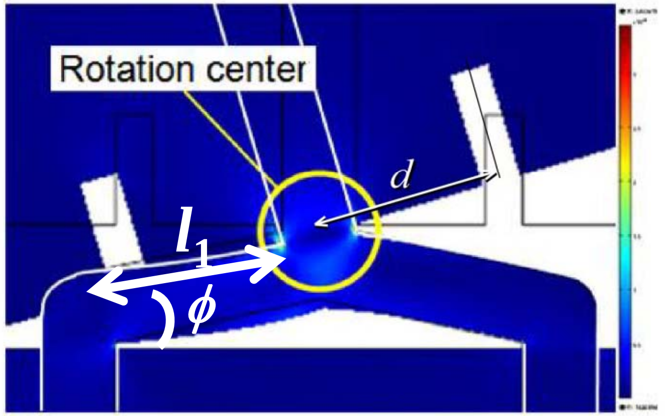

- **Wire decoupling**
- **Large movable angle**

Required accuracy: 50 μm

Wire-electric discharge machining

Gripper Design

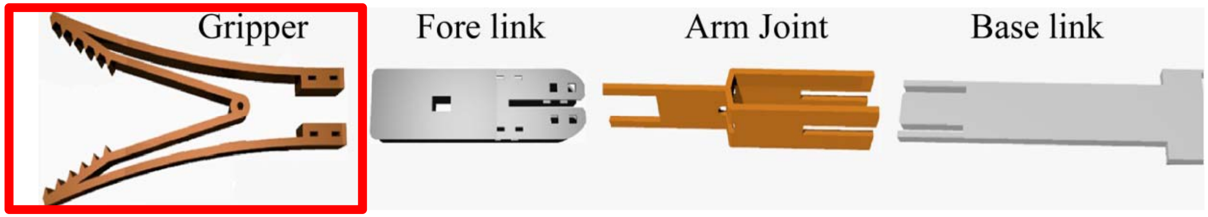

Pillar buckling

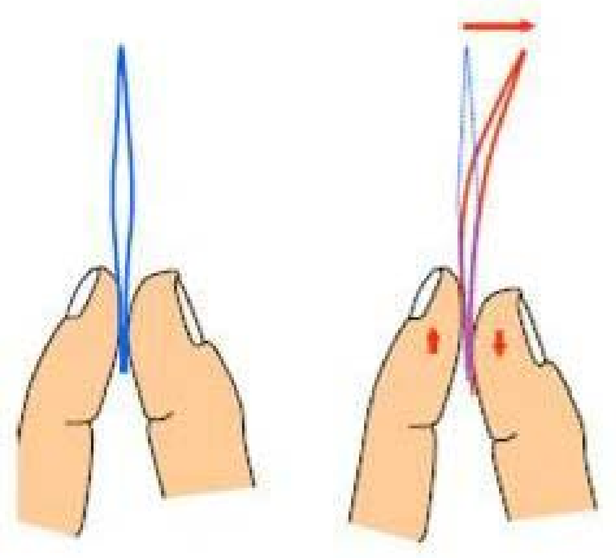

Muramatsu et al. (2000)

Without large mechanical elements

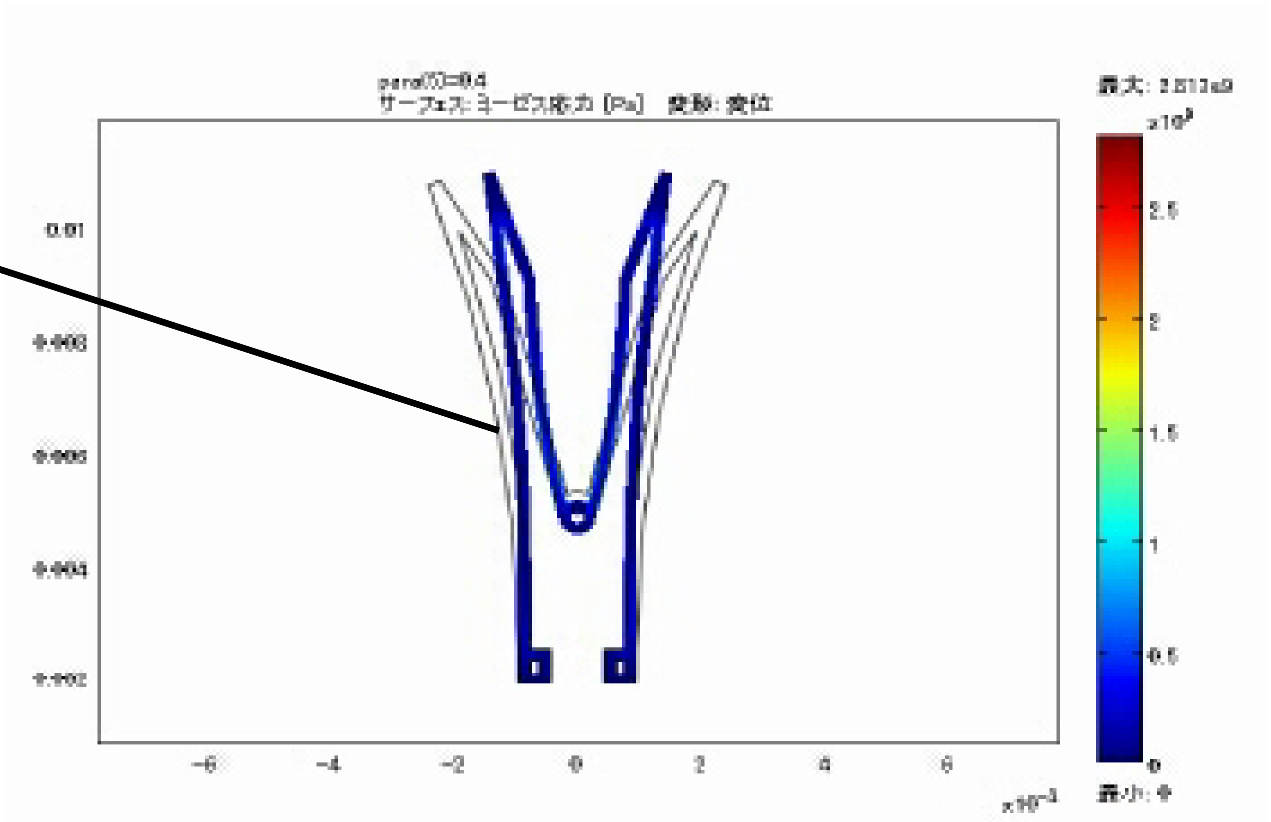

Normally-open type Gripper

Fabrication Process

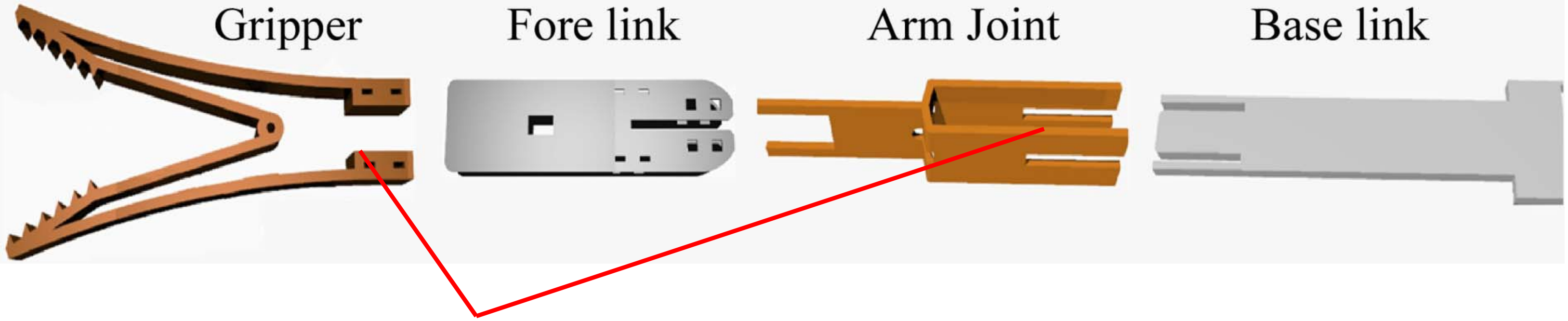

Wire-electric discharge (Phosphor bronze: thickness 1 mm)

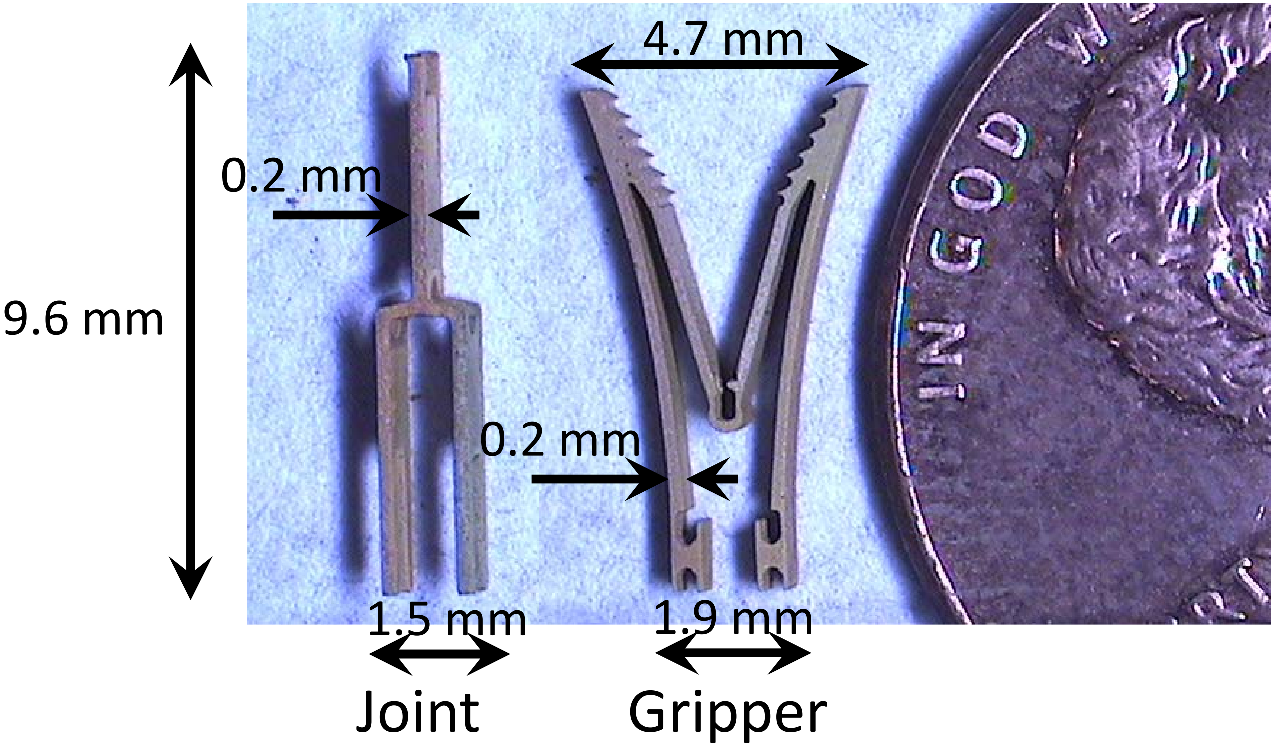

Fabrication Process

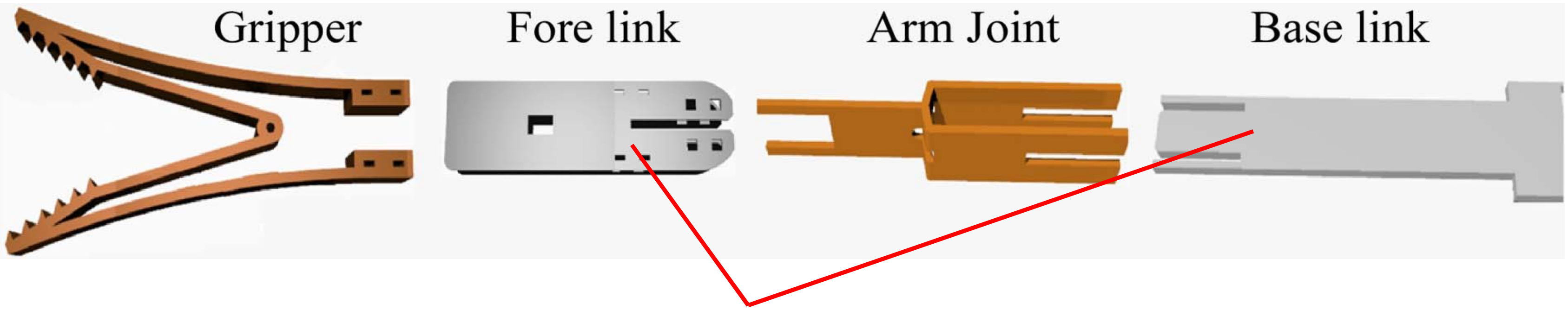

Photolithography + Electroplating

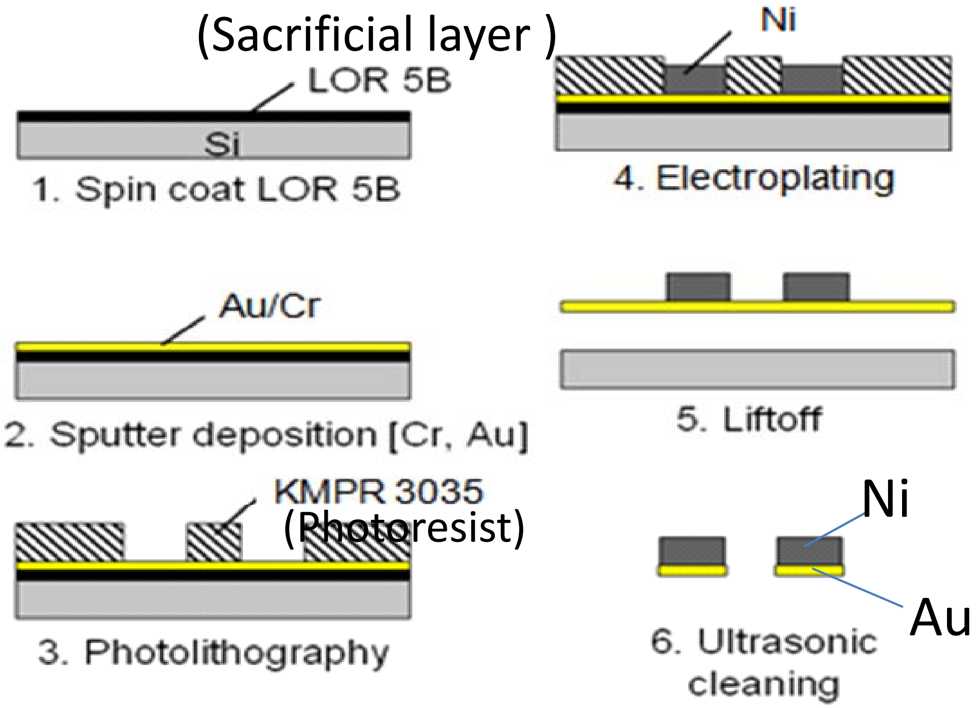

(Nickel: thickness 0.1 mm)

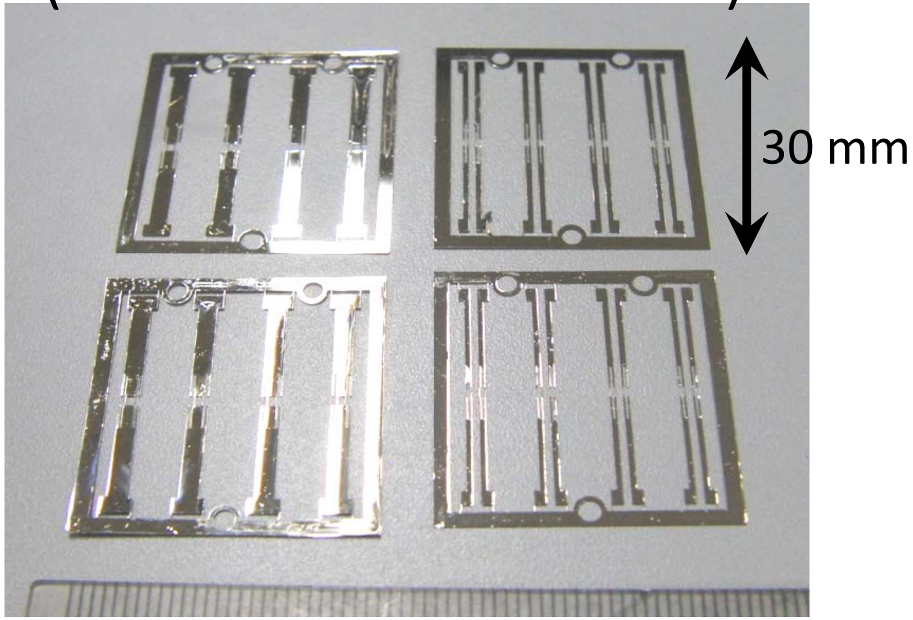

Fabrication Process

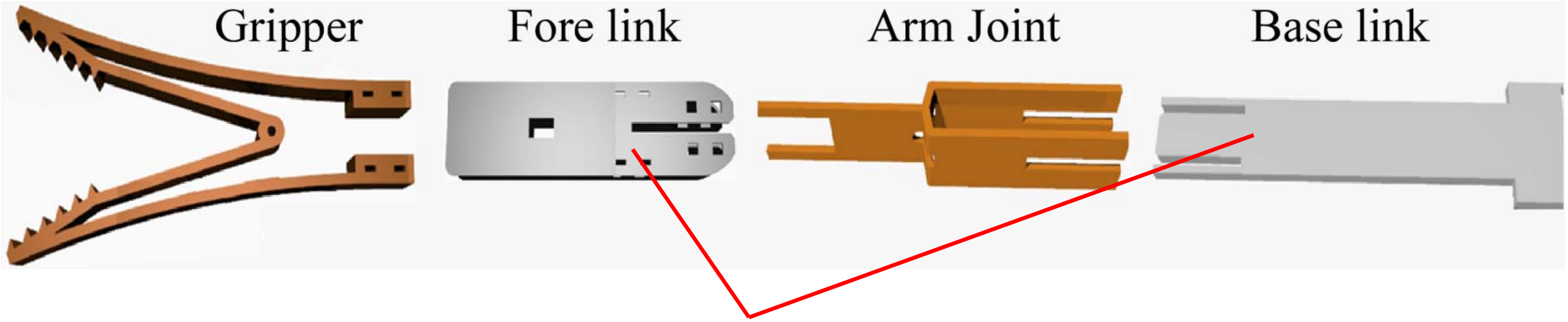

Photolithography + Electroplating

STAMP [Arai et al. JRM, 2009]

(Stacking Microassembly Process)

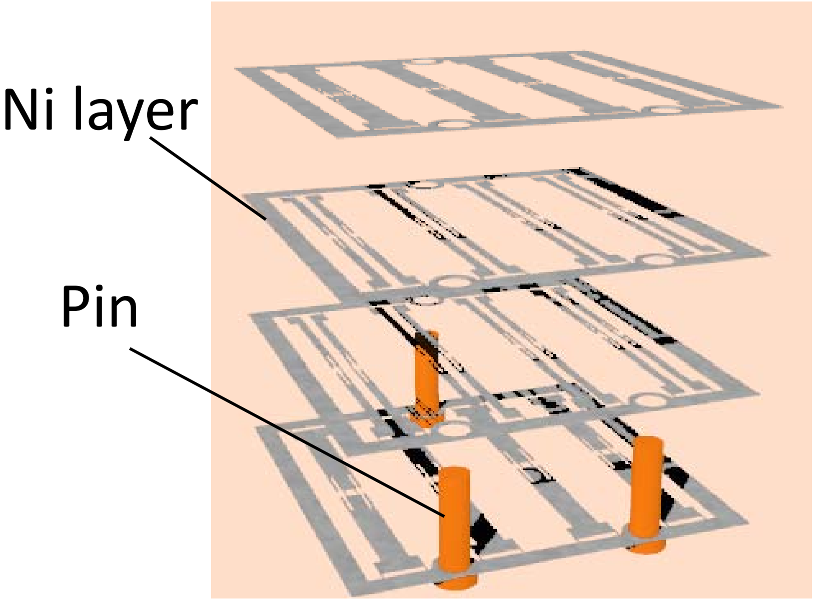

4 layers

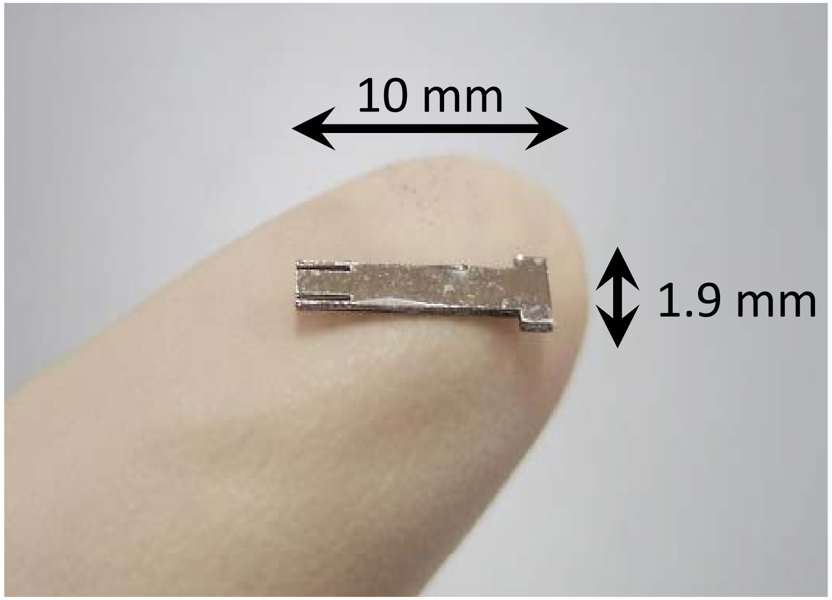

Animal Experiment

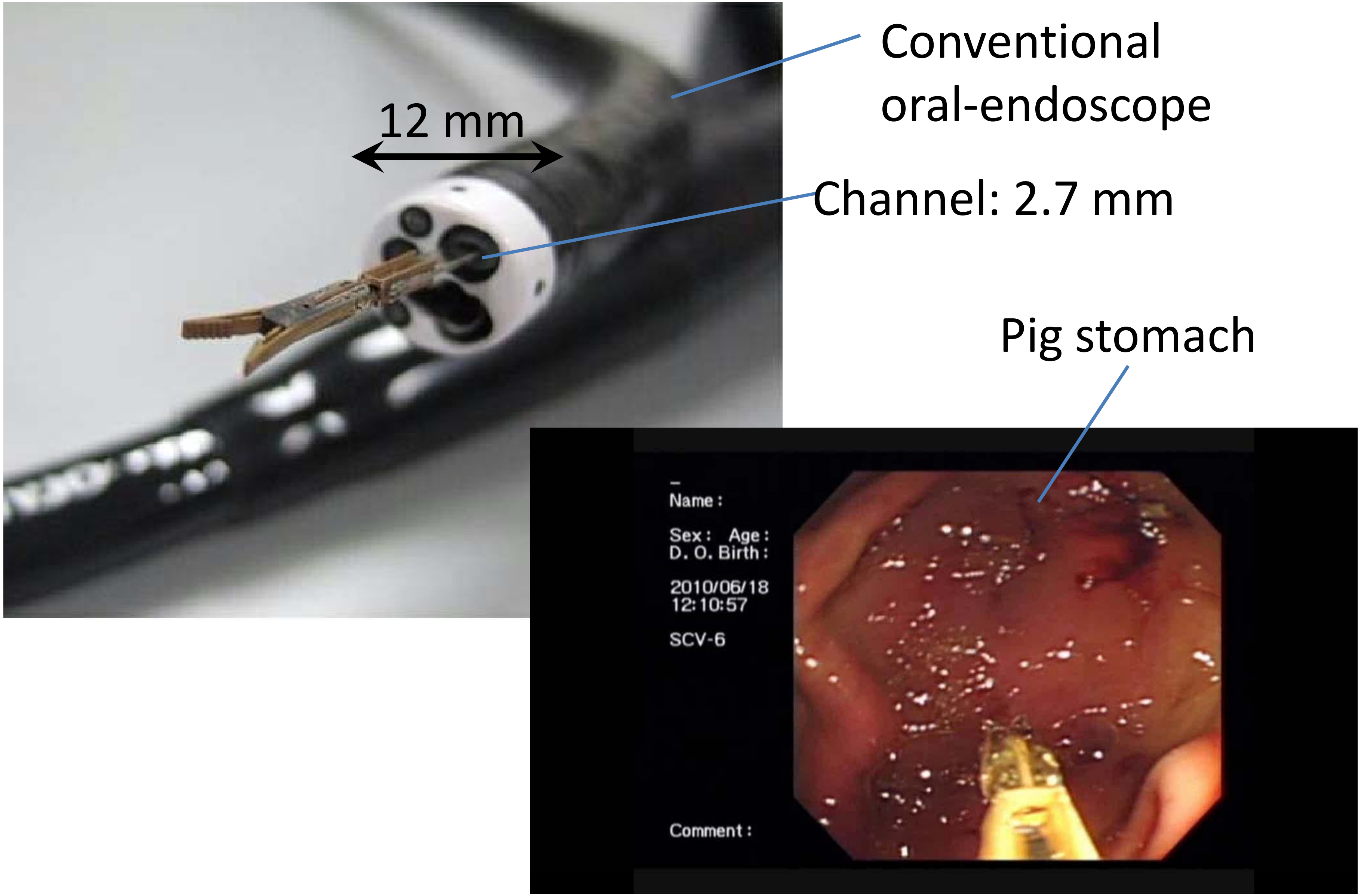

Application Examples

- Industrial Field -

Background

Needs a load sensor for robotics and healthcare field.

Tank(20 L):
80 kPa

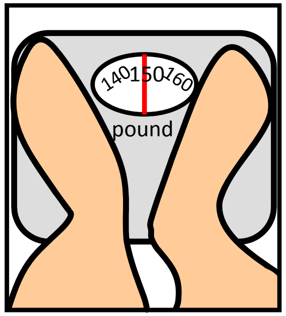

Weight:
20 kPa

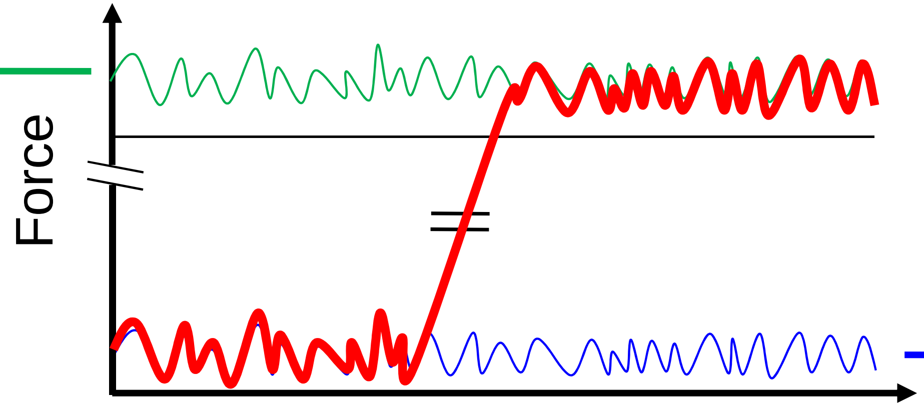

¥1coin:
86.5 Pa

Pulse

High sensitivity load sensing with a condition that compression force acted.

Expected characteristics :
1. Wide range measurement
2. Measuring a tiny variation with initial load

⇨ New principal, New type load sensor

Comparison of Conventional Load Sensors

Load Sensor Elements

- Strain Gauge
- Compressive Conductive Rubber
- Vision Sensor
- Piezoelectric Element
- Quartz Crystal

For wide range measurement,
we selected Quartz Crystal.

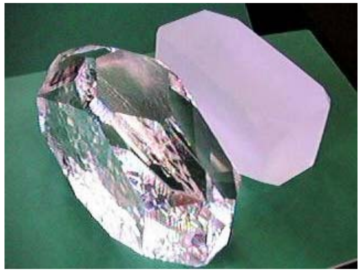

Artificial Crystal

http://www.tew.co.jp

Quartz Crystal type force sensor

- Sensing depends on the stress of the element.
- Robust against time and temperature change…

  High sensitivity & wide range measurement

  Excellent stability
- High frequency characteristic … High-speed measurement
- Self-vibration… Self-sensing function

Disadvantage: QCRs are vulnerable to stress concentration in bending.

Conventional Sensors

Comparison with Commercial Product and Previous Work

	(a) KISTLER 9001A 	(b) KISTLER 9207 	(c) Z. Wang et al. 2004 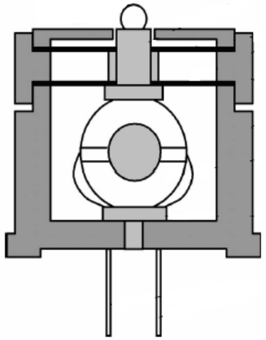
Output	Electric Charge	Electric Charge	Frequency
Measuring Objects	Quasi-static ~ Dynamic	Quasi-static ~ Dynamic	Static
Sensitivity	4 pC/N (1 g)	115 pC/N (50 mg)	105 Hz/N
Measuring Range	~ 7.5 N	±50 N	~ 100 N
Size [mm]	ϕ10.3 x 6.5	ϕ11.9 x 63.7	31 x 30 x 35

Our goal is to make sensitive, wide range, small (thin) load sensor using AT-cut quartz crystal resonator.

Concept of Load Sensor

Characteristics of Vertical Type Load Sensor

1. Resolution improvement
 ⇒Vertical type maintenance
2. Stable maintenance
 ⇒Blade spring
 and outer casing
3. Further miniaturization
 ⇒$\phi 7 \times 11$ mm
 (1/4 volume ratio)

Packaging: more compact
$V_1 = \pi \times 3.5^2 \times 11 \text{ mm}^3$
$V_2 = \pi \times 6.5^2 \times 13 \text{ mm}^3$
$V_1 / V_2 \fallingdotseq 0.25$

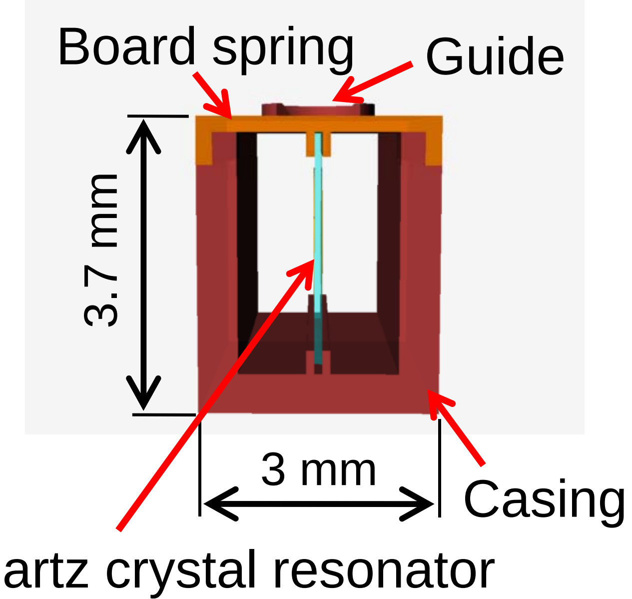

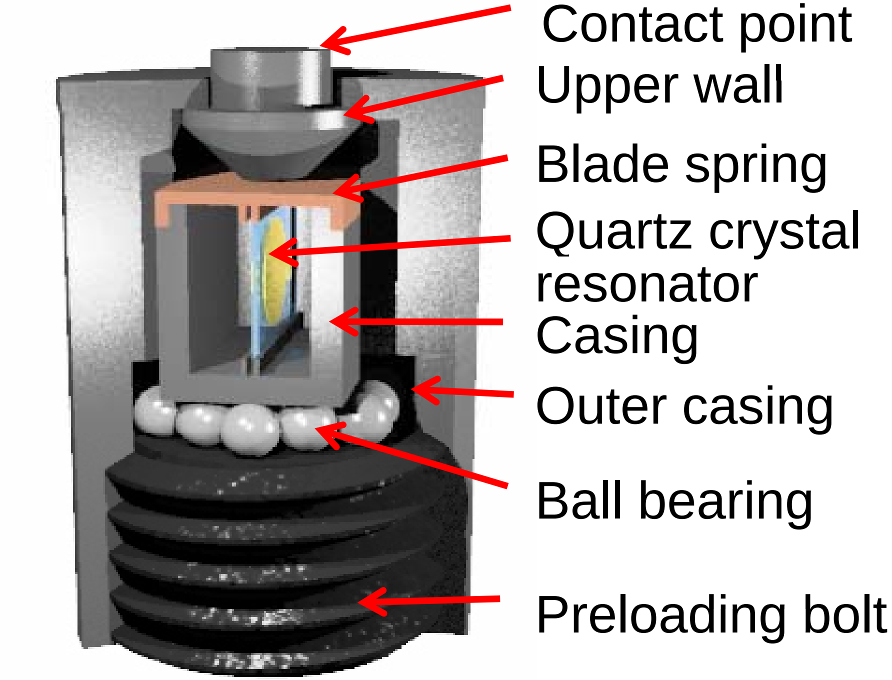

ϕ7 mm x 11 mm

Ref.) Narumi et al., JRM, 2009

Structural Analysis

Stress distribution in z axis

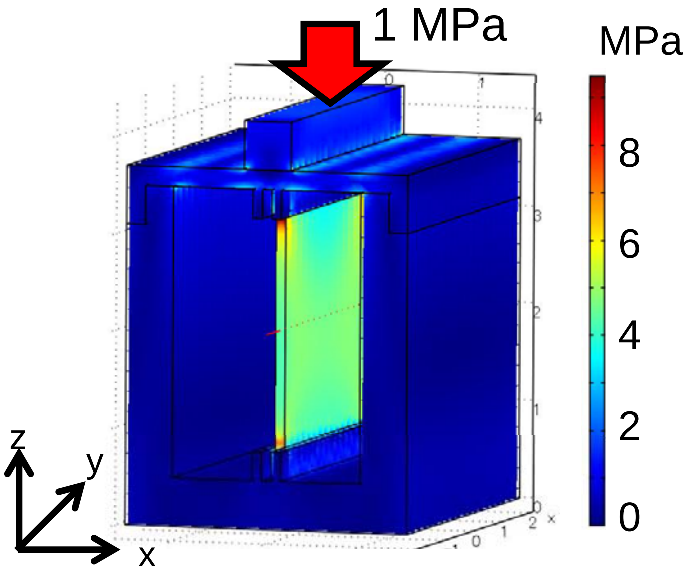

Load Conversion Efficiency

Section area of QCM　: 0.1 mm x 3 mm = 0.3 m

Impressed load to QCM : 4.7 MPa x 0.3 mm^2 = 1.41 N

⇒Load Conversion Efficiency : 1.41 / 2.0 = 0.705

cf. Load conversion efficiency of conventional sensor was 0.37.

Stress distribution in y axis

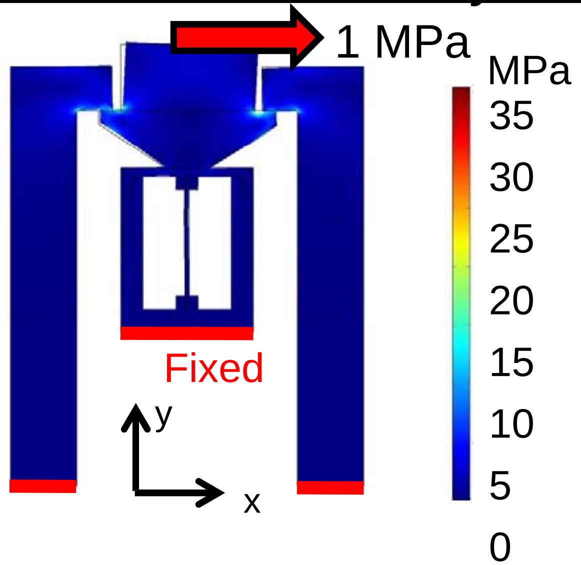

Displacement distribution in y axis

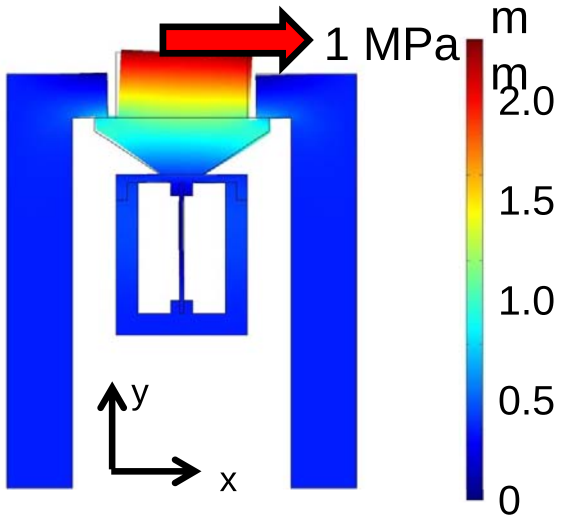

Fabrication -Quartz Crystal Resonator-

Concept of Quartz Crystal Resonator

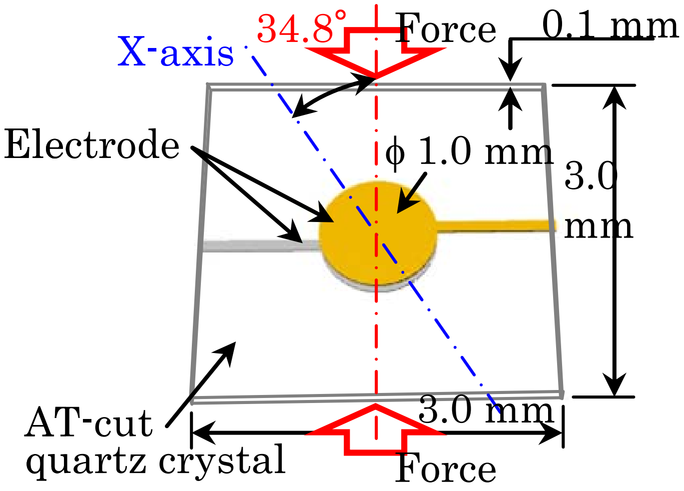

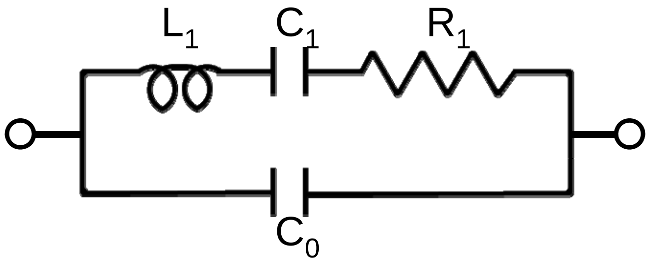

Equivalent circuit

Fabrication Process

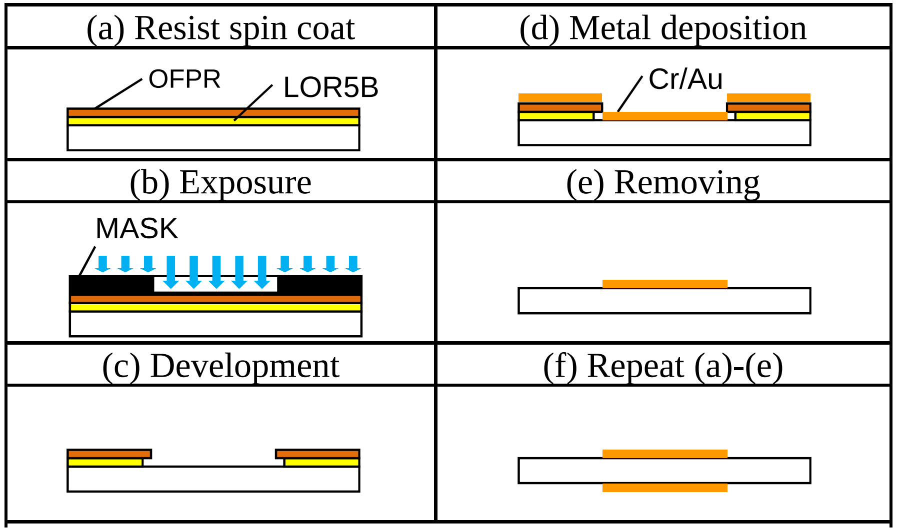

Fig. 8 Fabrication process of QCR.

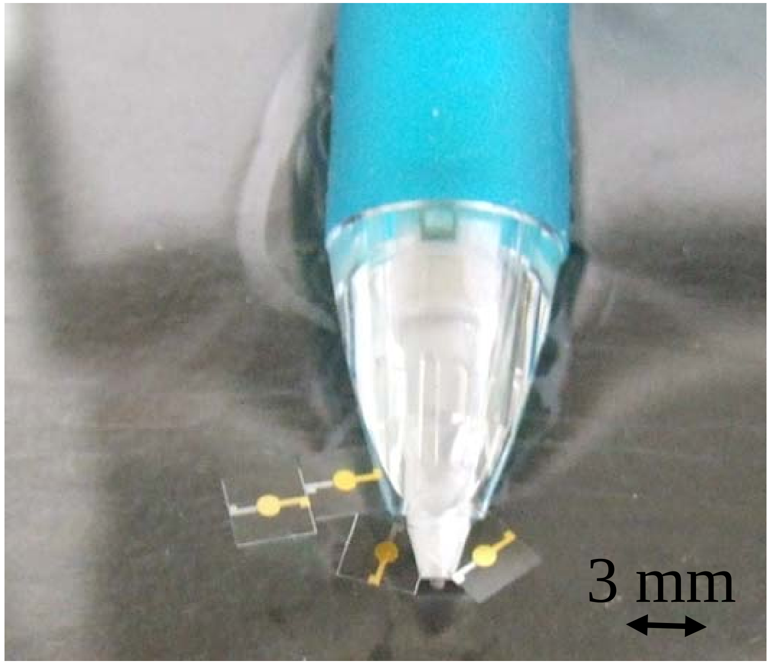

Fabricated quartz crystal resonator

Fabrication -Retention Mechanism-

Fabrication of Retention Mechanism

Fabrication method: Wire electrical discharge machining
Material -Casing: SUS304
-Blade Spring: Phosphor bronze

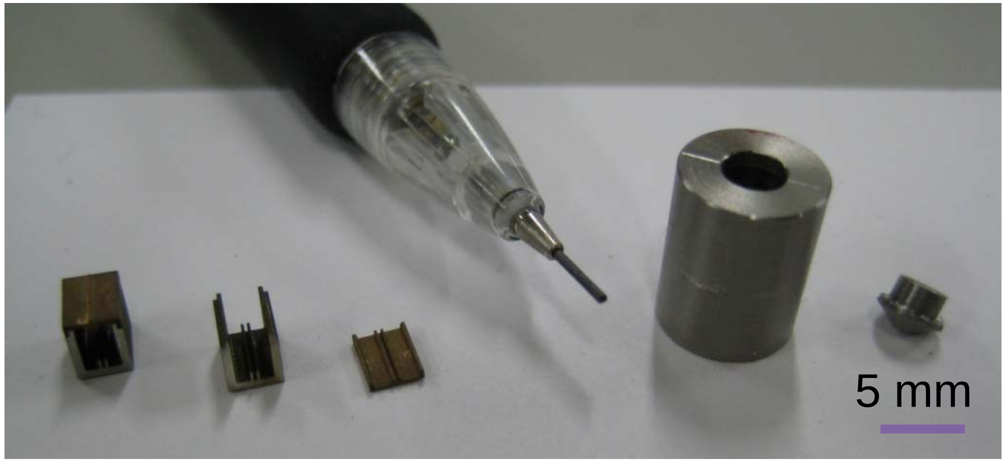

Fabricated retention mechanism and casing

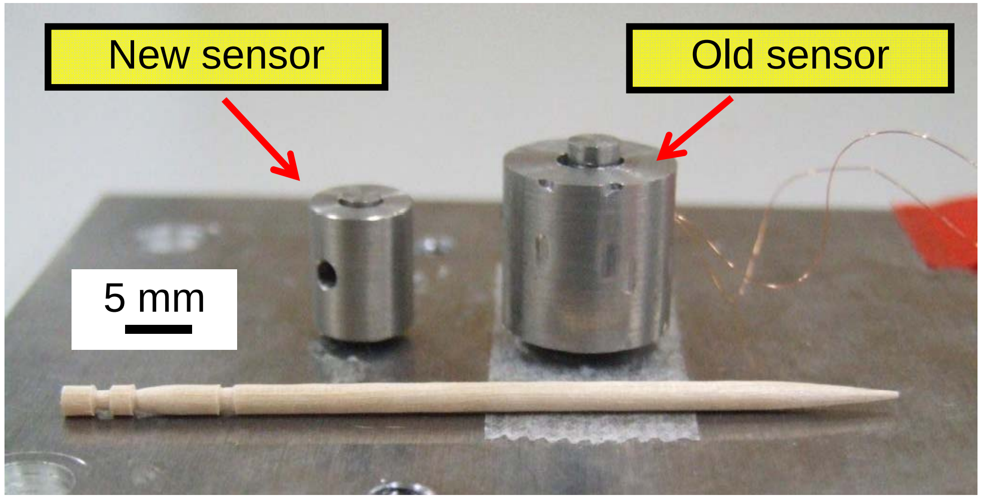

Comparison with conventional sensor’s package

Loading Experiment with Package

Experimental Setup

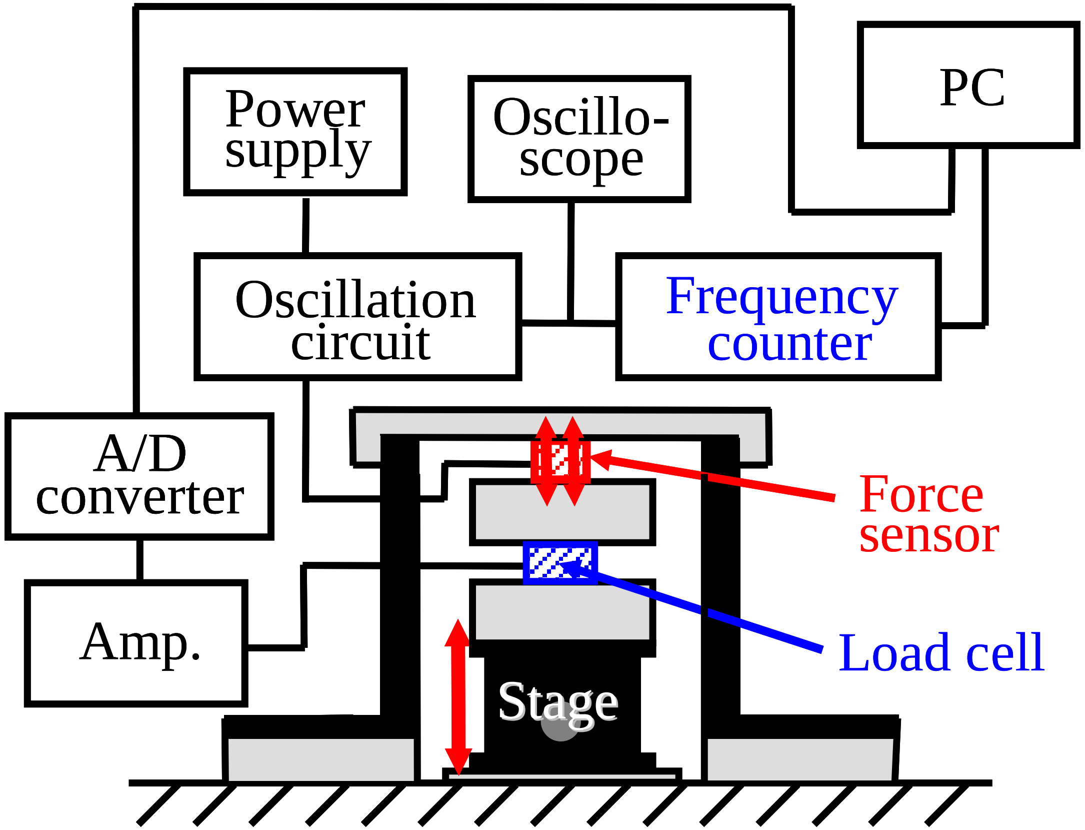

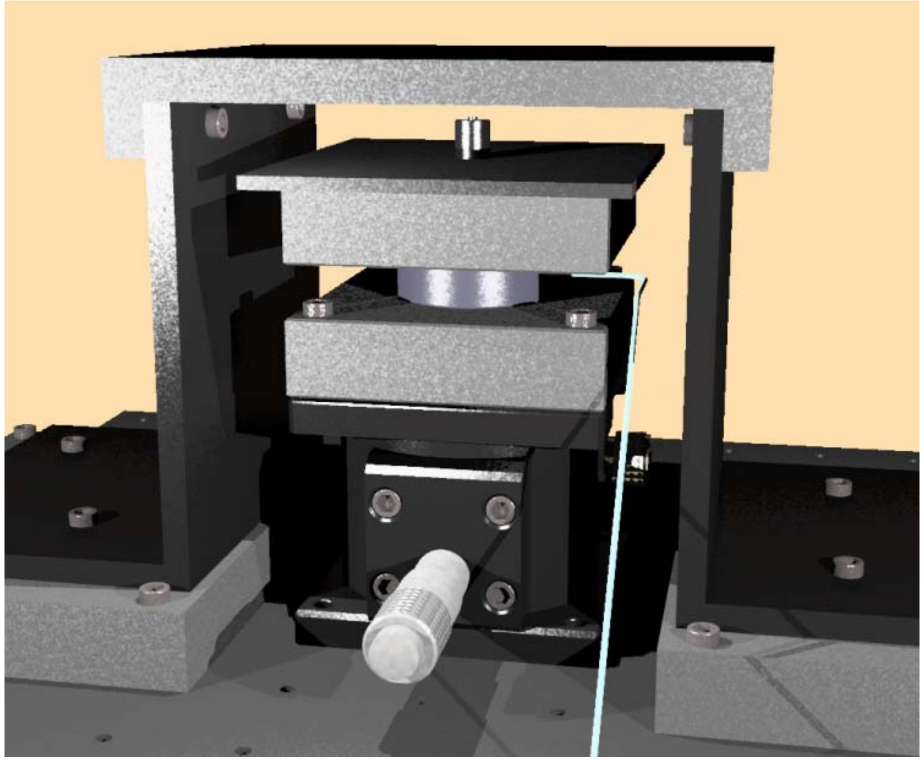

1. The sensor is pressed to wall by moving Z stage vertically.
2. The load given to the sensor is measured by load cell as the sensor and load cell are placed vertically.
3. Sensor output (resonance frequency) was measured by frequency counter.

Experimental Results

With no Initial Load

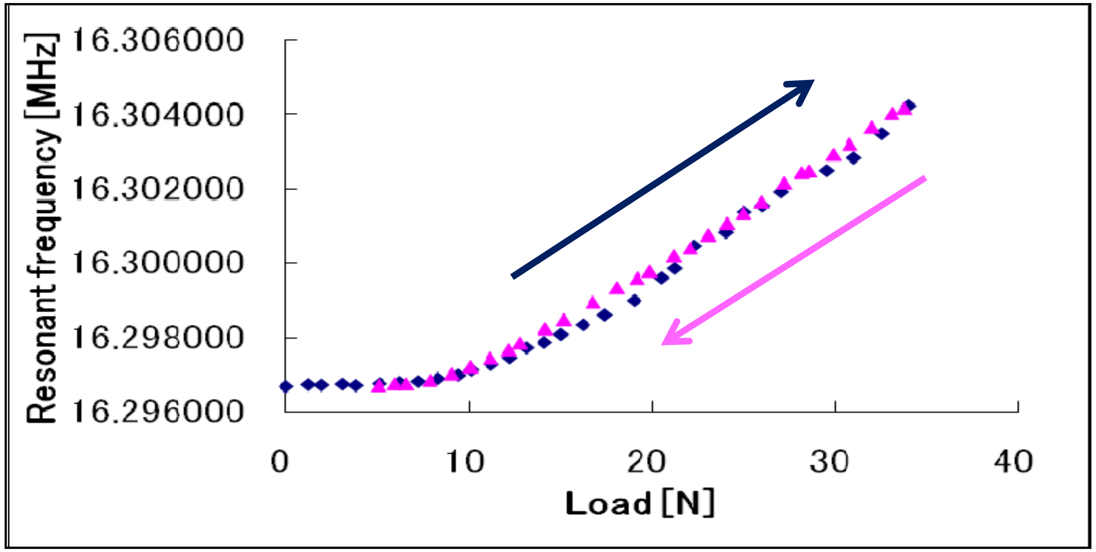

Experiment condition

Temperature : 22℃
Humidity : 45%
Voltage : 4.5 V

With Initial Load of 10 N

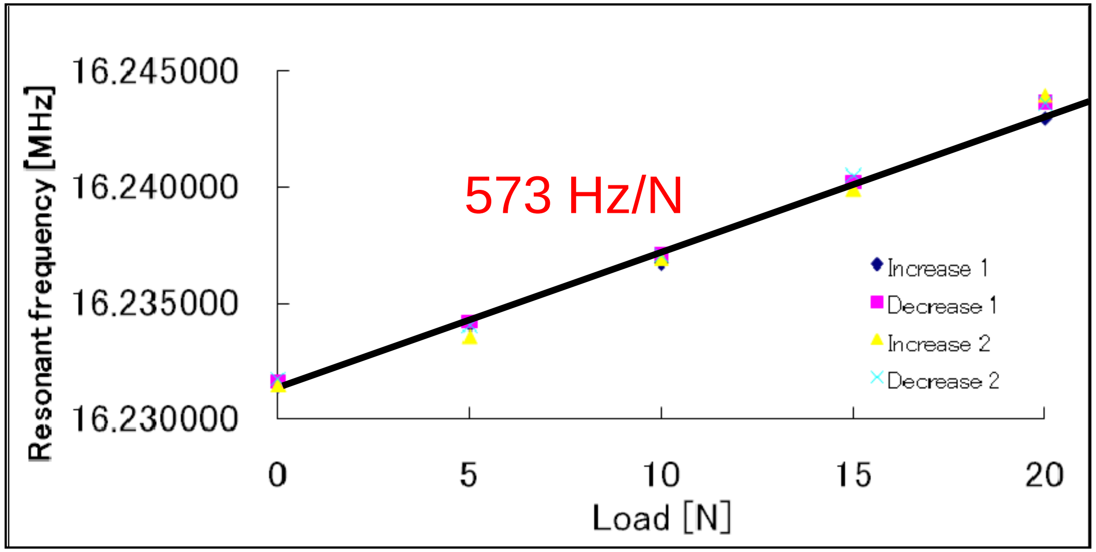

Experiment condition

Temperature : 25℃
Humidity : 45%
Voltage : 4.5 V
Initial load is 10 N

$Y = 573.0 \times 10^{-6} X + 16.231$
$R^2 = 0.9452$
X : Load [N]
Y : Resonant frequency [MHz]

Discussion

Allowable stress to QCM is 128 MPa (38.4 N).

Resolution of the new type force sensor is seven times to the conventional one. (1250 / 160 = 7.8, 215 / 30 =7.2)

	New type sensor	Conventional type sensor
Force conversion efficiency	70 %	37 %
Maximum load	38.4 x (100 / 70) = 54.9 N	38.4 x (100 / 37) = 103.8 N
Resolution	3.21 mN (0.33 g)	22.5 mN (2.30 g)

Comparison to measurement range

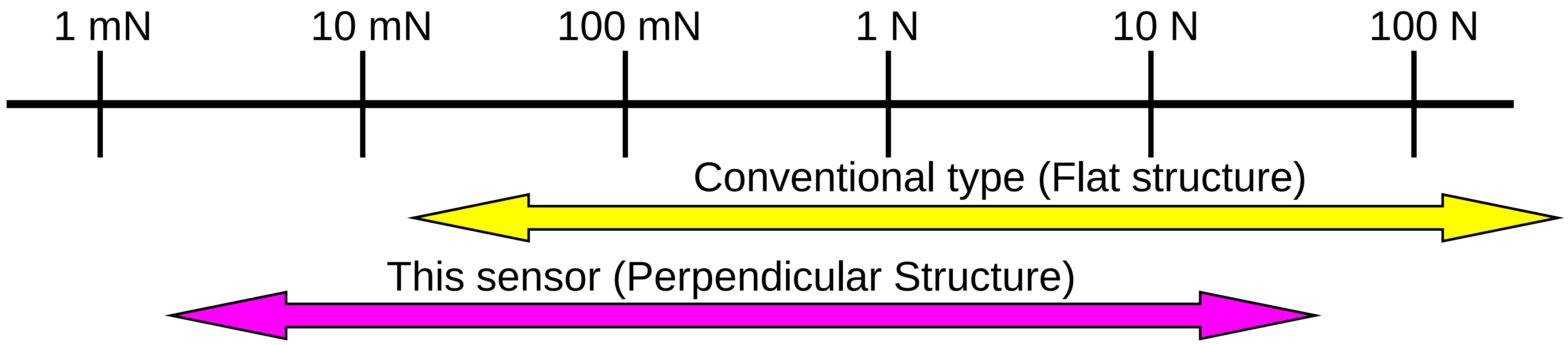

Application Examples

- Fundamental Research Field -

Background

Temperature measurement for nanoscale object

Cantilever
with
a carbon
nanotube
(CNT)

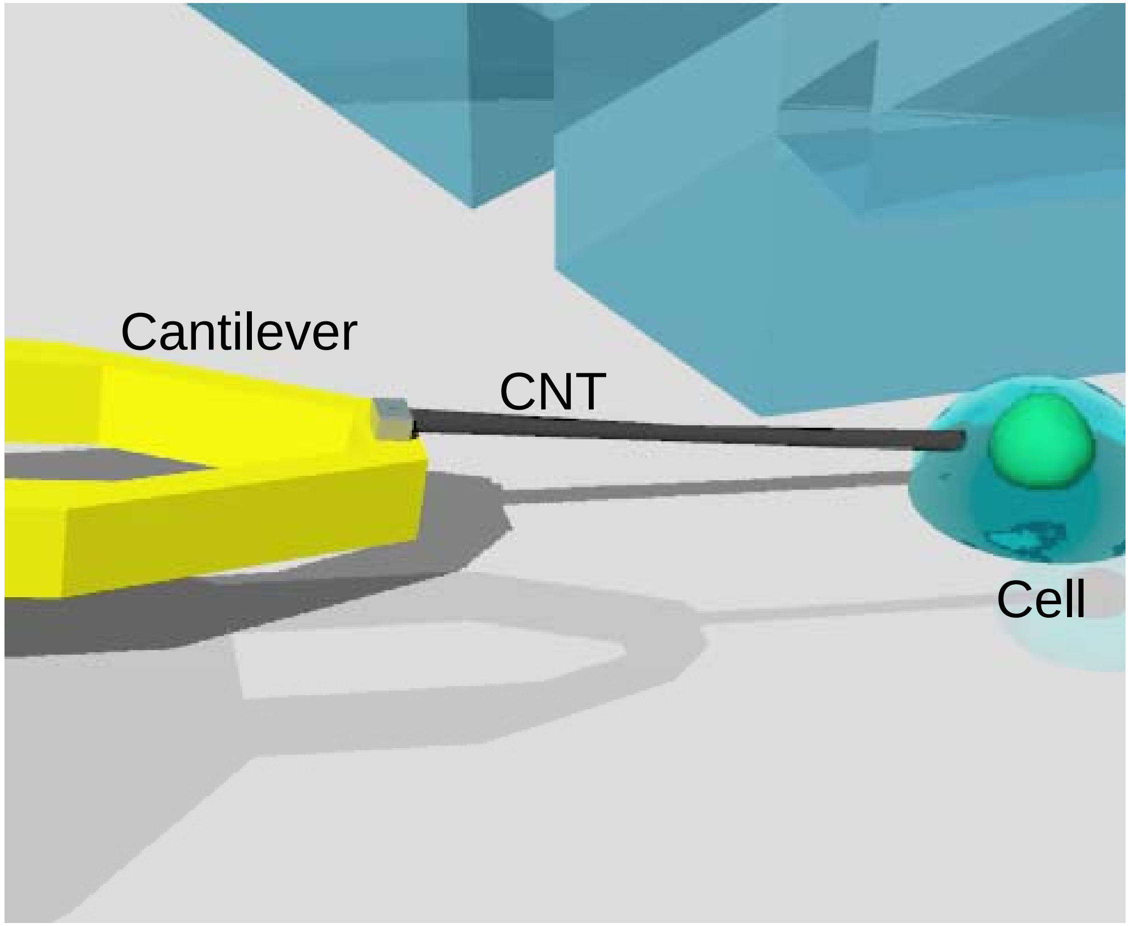

➡ Employ carbon nanotube as a tip of cantilever

CNT

Why CNT？

Graphene sheet with a cylindrical nanostructure

Ex) Single wall, Double wall, Multi wall carbon nanotube

- Small size (on the order of a few nanometers in diameter)

- High heat conduction (3000～6000 W/m･K), (cf：Cu 400 W/m･K)

- High stability

- High strength (up to 48,000 kN·m/kg),
  (cf: high-carbon steel's 154 kN·m/kg)

- High current density tolerance (10^9A/cm^2)
  (cf ：Cu10^6A/cm^2)

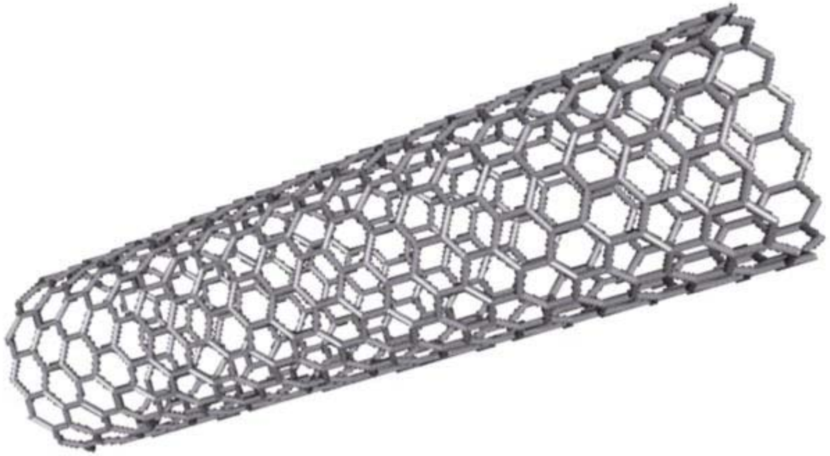

http://www.aero.kyushu-u.ac.jp/aml/fig/cnt.jpg

Thermal property of CNT

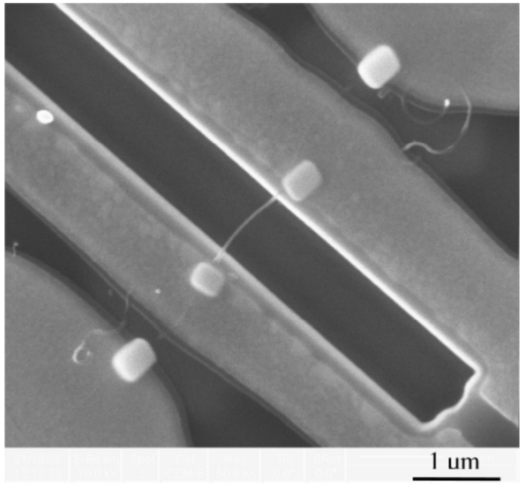

300 W/mK

T.Y. Choi, et al, NANO LETTERS, Vol. 6, No. 8, 1589-1593, 2006.

100 – 700 W/mK

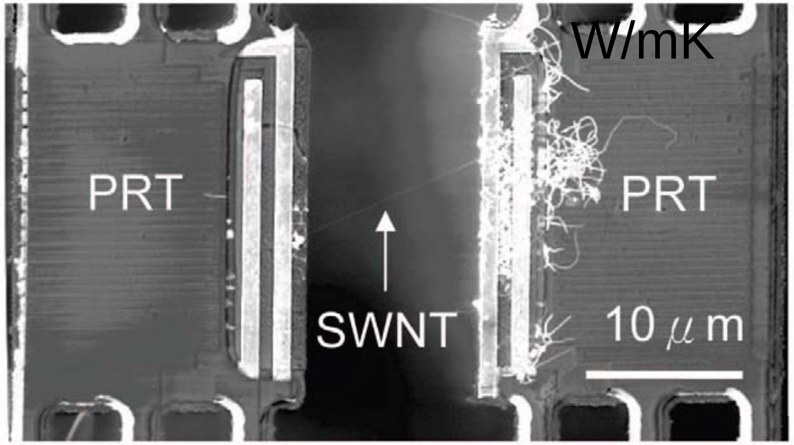

I.K. Hsu, et al, NANO LETTERS, Vol. 9, No. 2, 590-594, 2009.

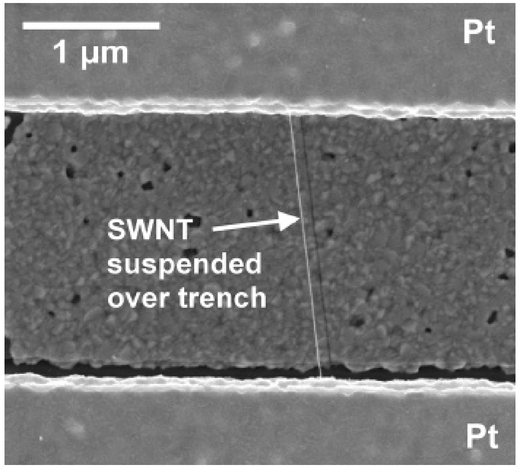

3500 W/m K

E. Pop, et al, NANO LETTERS, Vol. 6, No. 1, 96-100,2006.

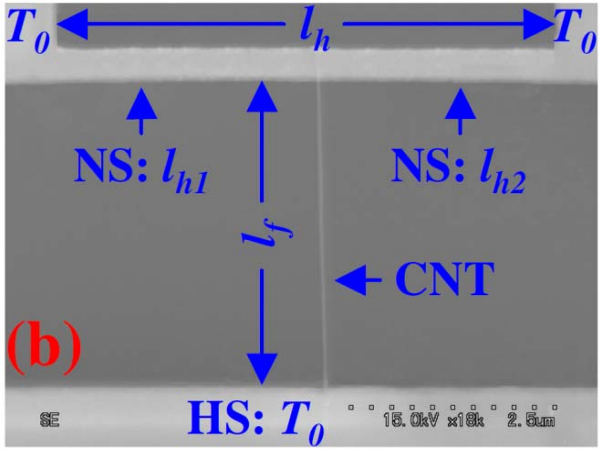

2000 W/m K

M. Fujii, et al, PHYSICAL REVIEW LETTERS, 95, 065502, 2005.

In vacuum

Purpose

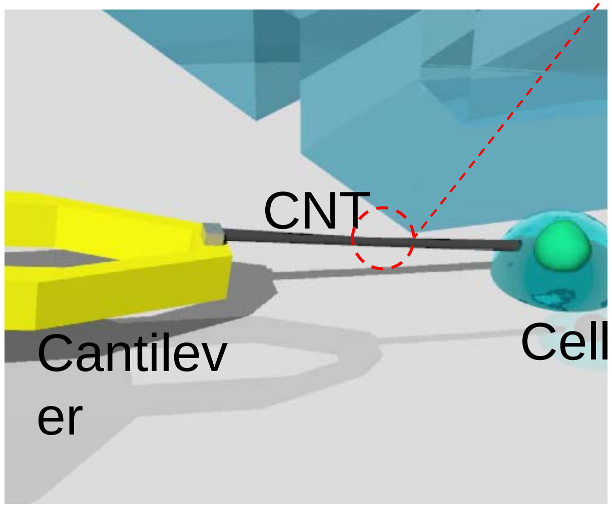

Problem

➡ High heat conduction (3000～6000 W/m･K)

Theoretical value

How about the flow of heat in water and air?

Purpose of this study

Evaluation of thermal characteristics of CNT in air and water

How much is the value of the heat flow of CNT actually in air and water?

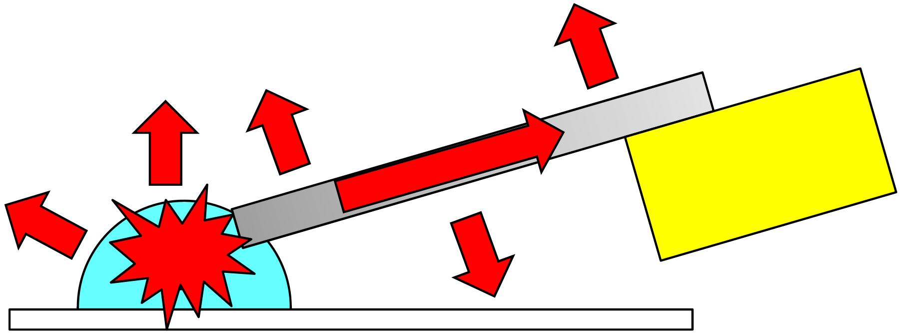

Purpose

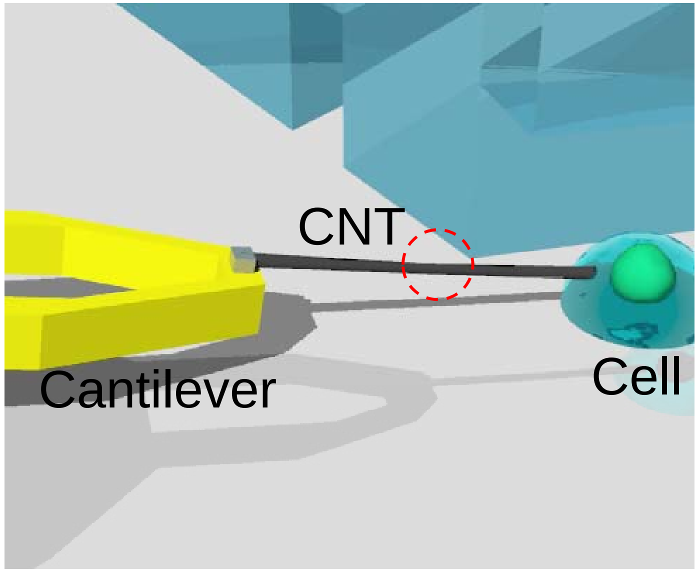

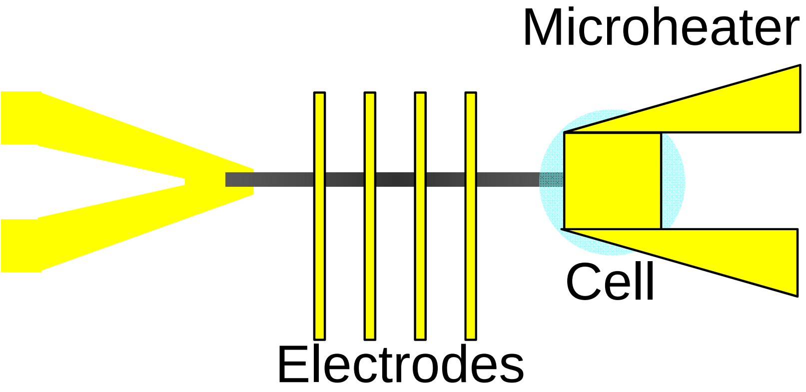

Point

Detecting heat from the end of CNT

1. Heating at the end of CNT

➡ Using microheater

2. Heat detection

➡ Measuring electrical resistance by 4-point method

Design

Pattern on wafer

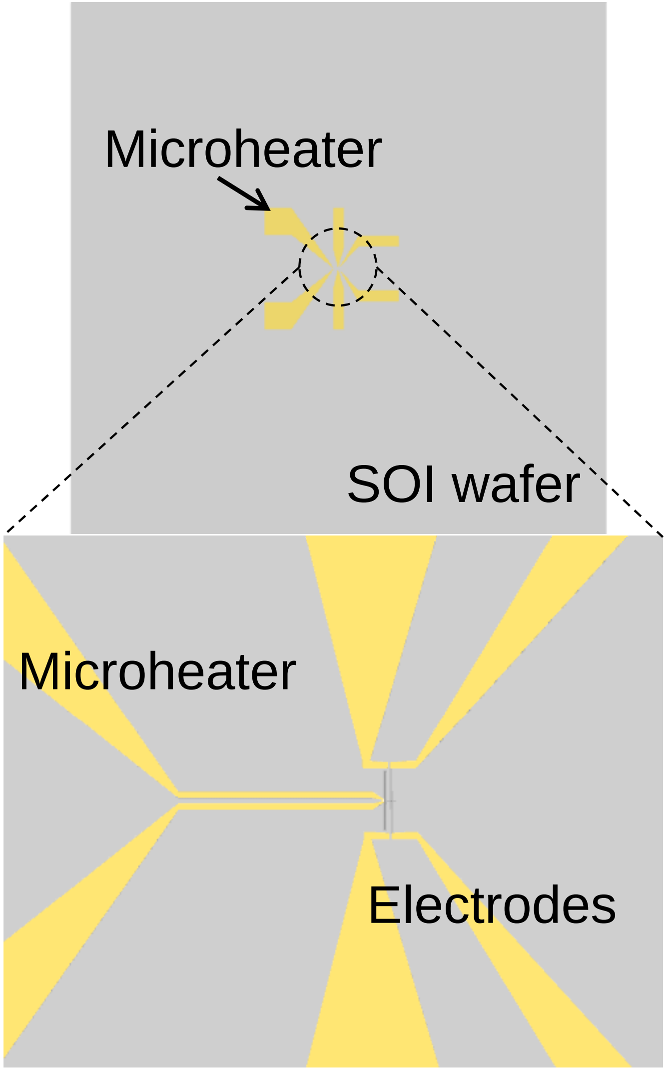

(a) Overall view

Chip size: 20 mm× 20 mm ×550 μm
(SOI Si:SiO2:Si = 1.5 μm:3 μm: 550 μm)
Gap: 1 μm× 50 μm ×5 μm

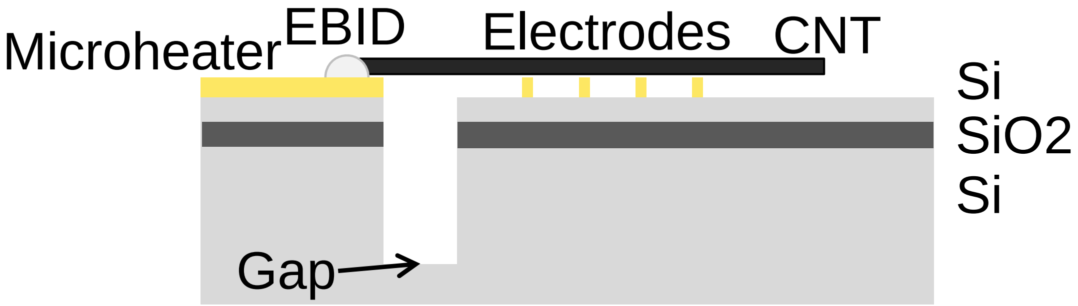

(c) Side view

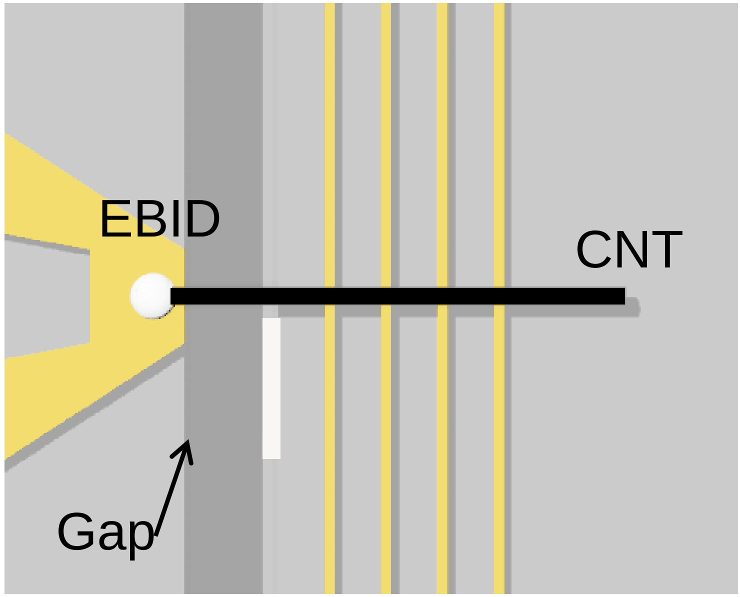

(b) Top view

Fabrication

Fabrication

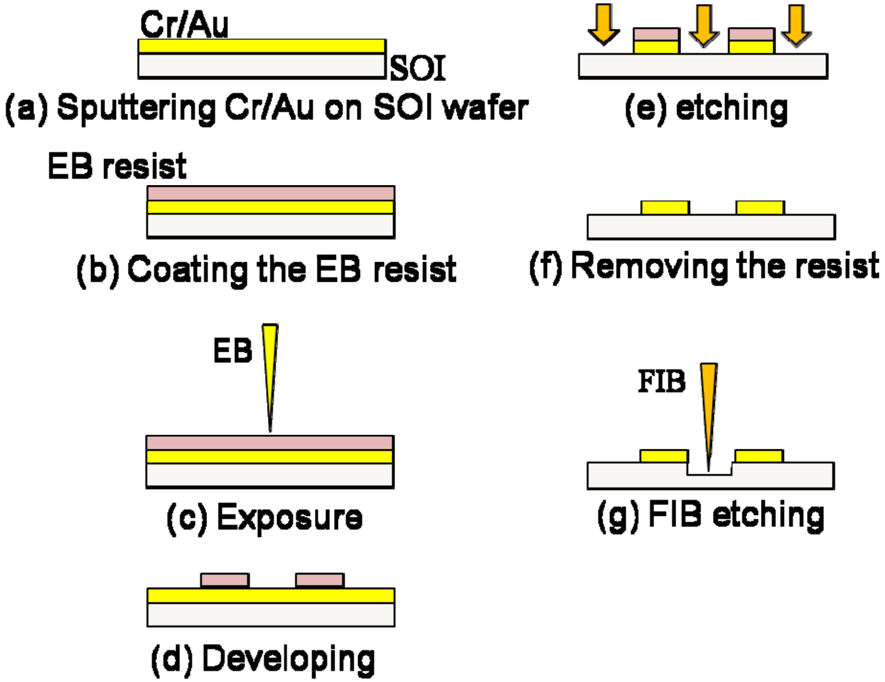

(a) Sputtering Cr/Au on SOI wafer

(b) Coating the EB resist

(c) Exposure

(d) Developing

(e) etching

(f) Removing the resist

(g) FIB etching

Fabrication process

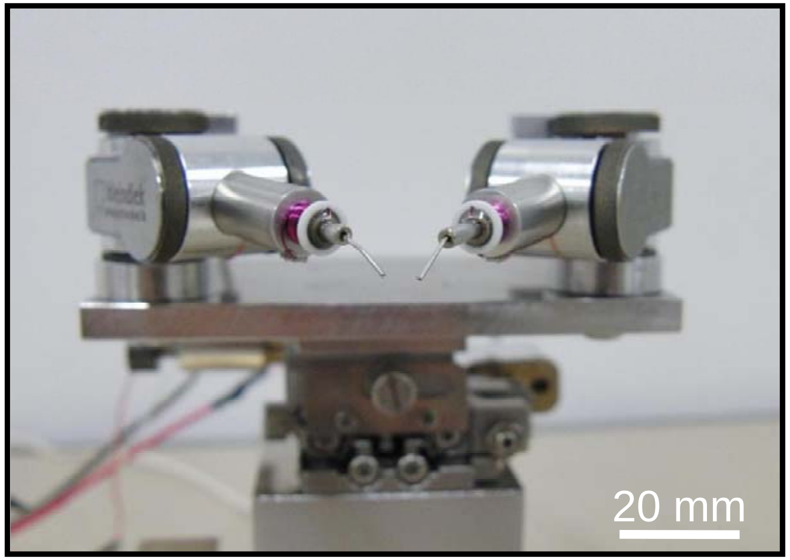

Nanomanipulator

(MM3A, Kleindiek Nanotechnik Gmbh)

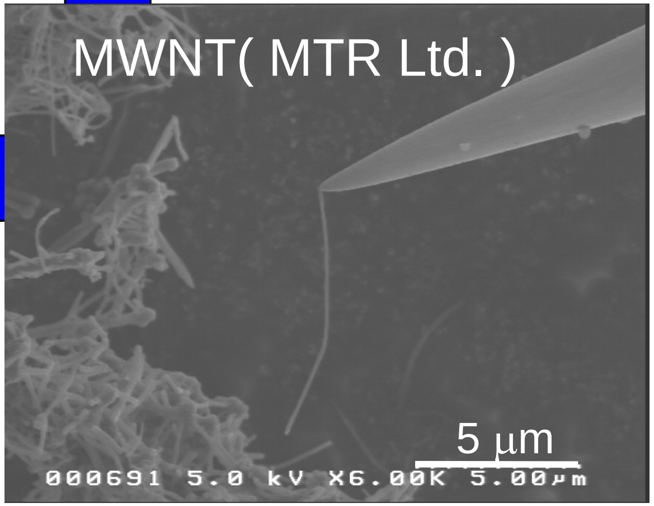

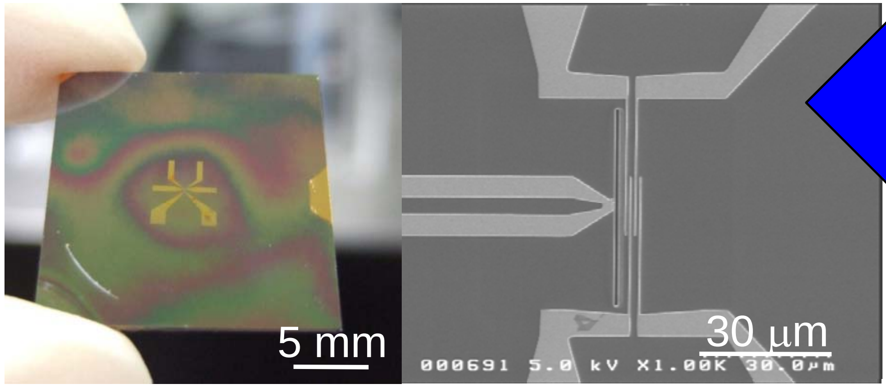

Fabricated pattern

Experiments

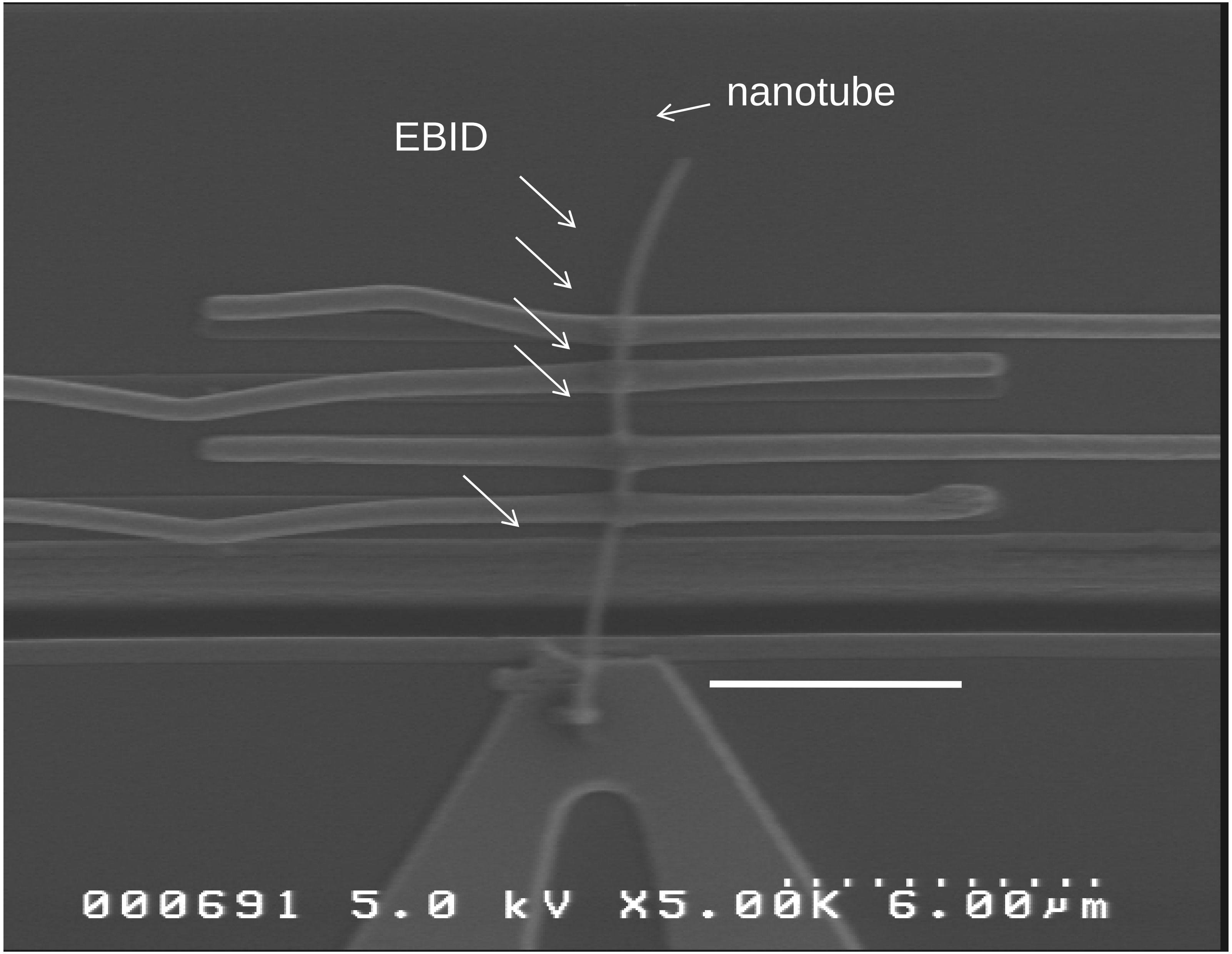

CNT on the pattern

Measured result (water)

Air

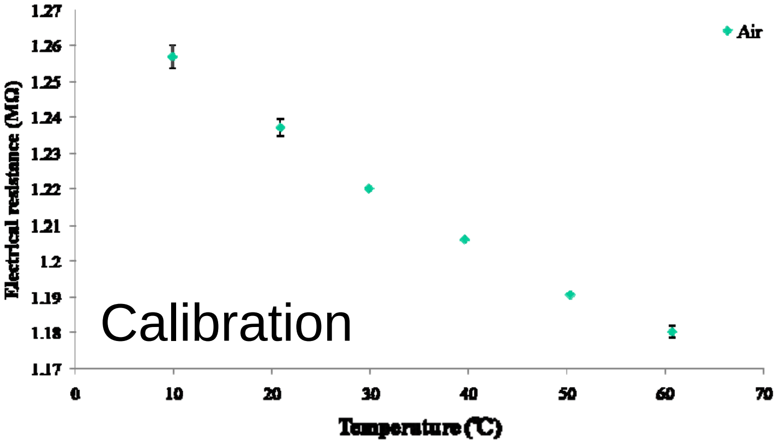

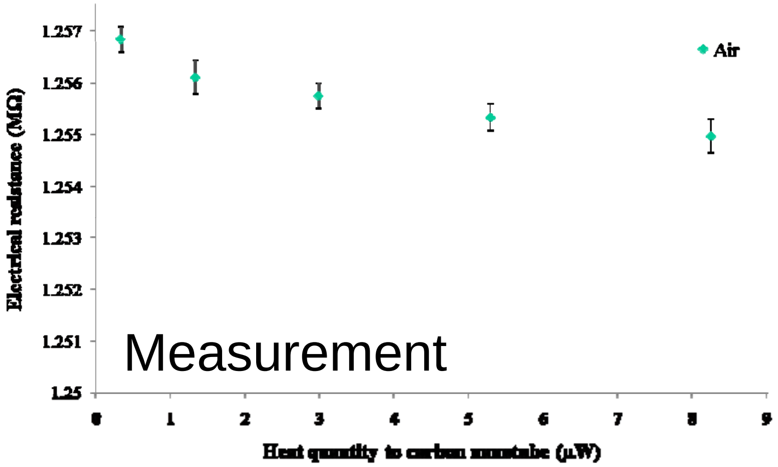

1.23°C/79.1 μJ

Water

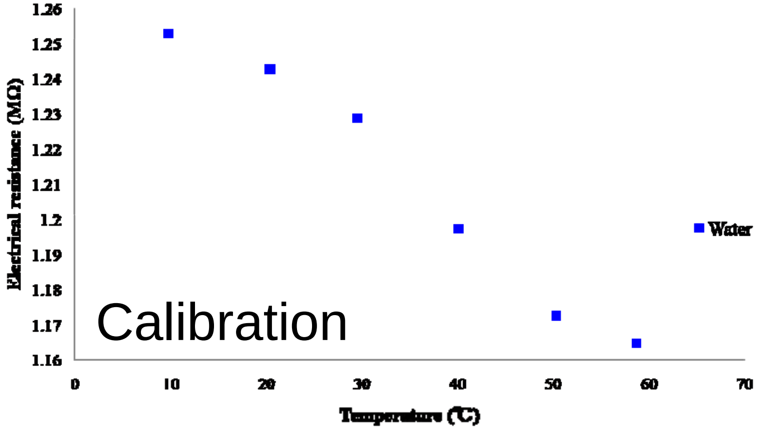

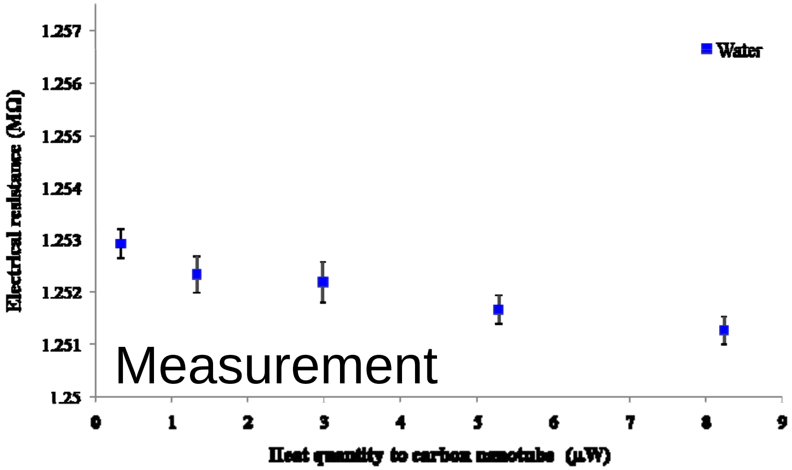

0.846 °C/79.1 μJ

Heat quantity to increase the temperature of CNT in water (93.8 μJ/K) was lower than that in air (64.3 μJ/K)

Application Examples

- Bio Field -

Background

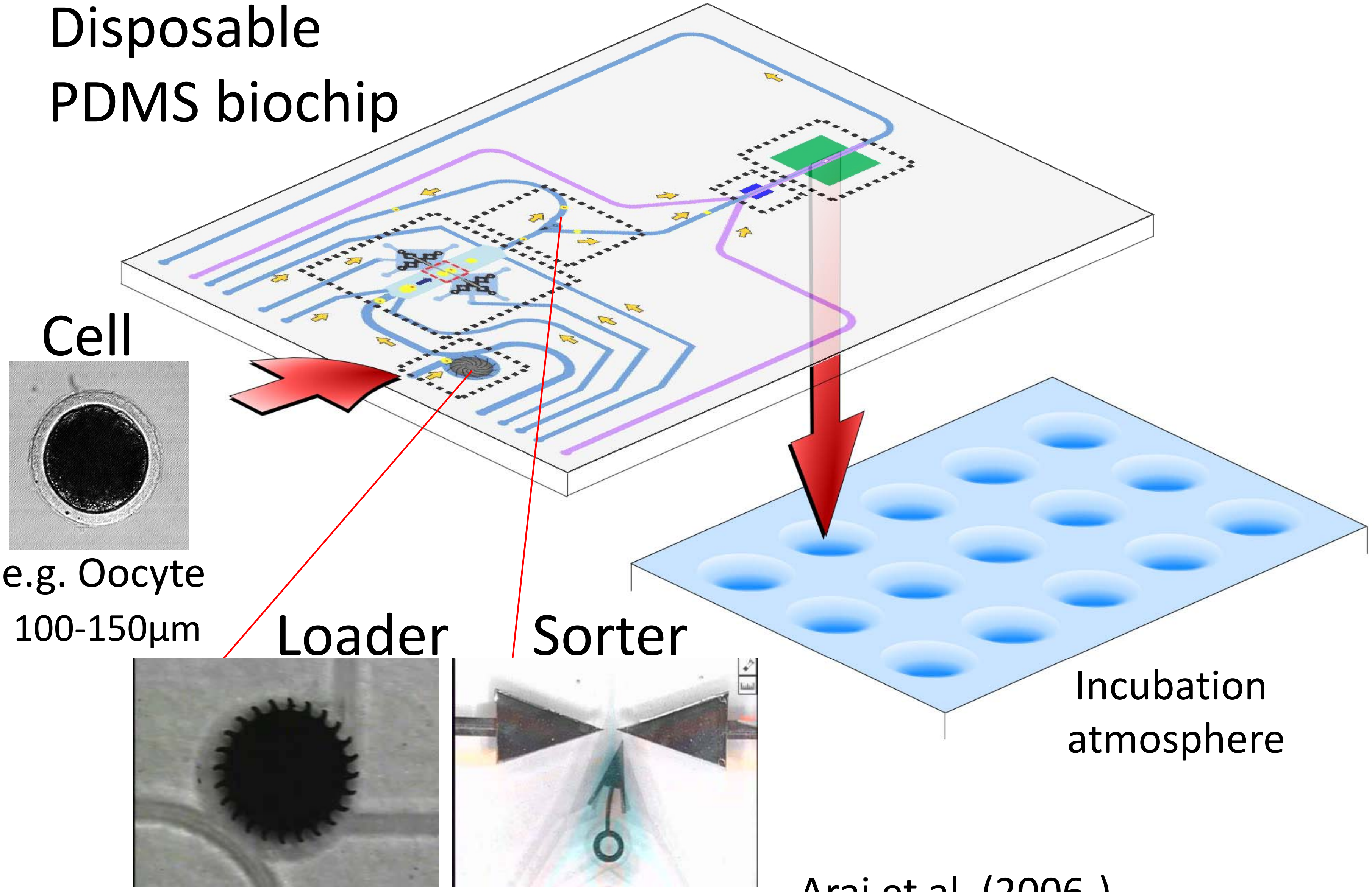

Disposable
PDMS biochip

Cell

e.g. Oocyte
100-150µm

Loader

Sorter

Incubation
atmosphere

Arai et al. (2006-)

Automation system of supplying cells one by one from biochip to incubation atmosphere is highly required.

Rerated Works

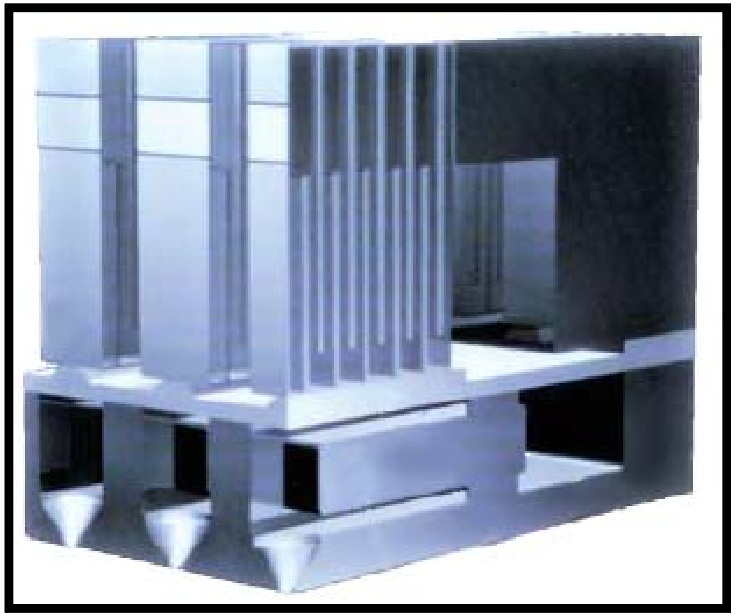

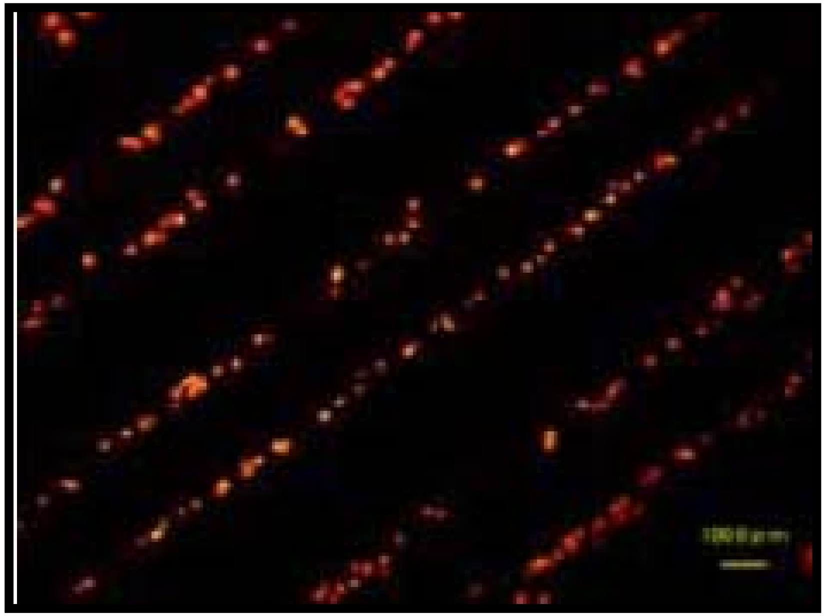

Inkjet mechanism (EPSON Co, Ltd.)   Bio-printing (Nakamura et al.)

Solution tank

Nozzle

Drive unit

Problems

- Cleaning
  (Contamination)
- Cannot dispense
  a single cell

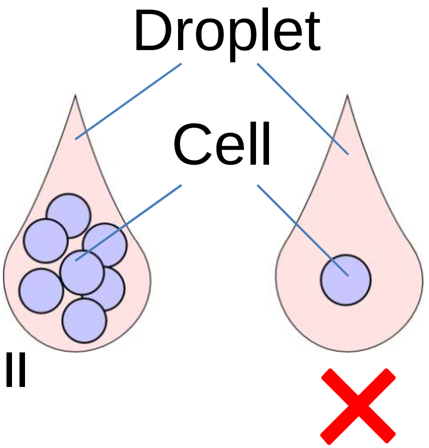

Automatic Cell Dispensing System for a single cell dispensing

Ref.) Kawahara et al., μ-TAS, 2010

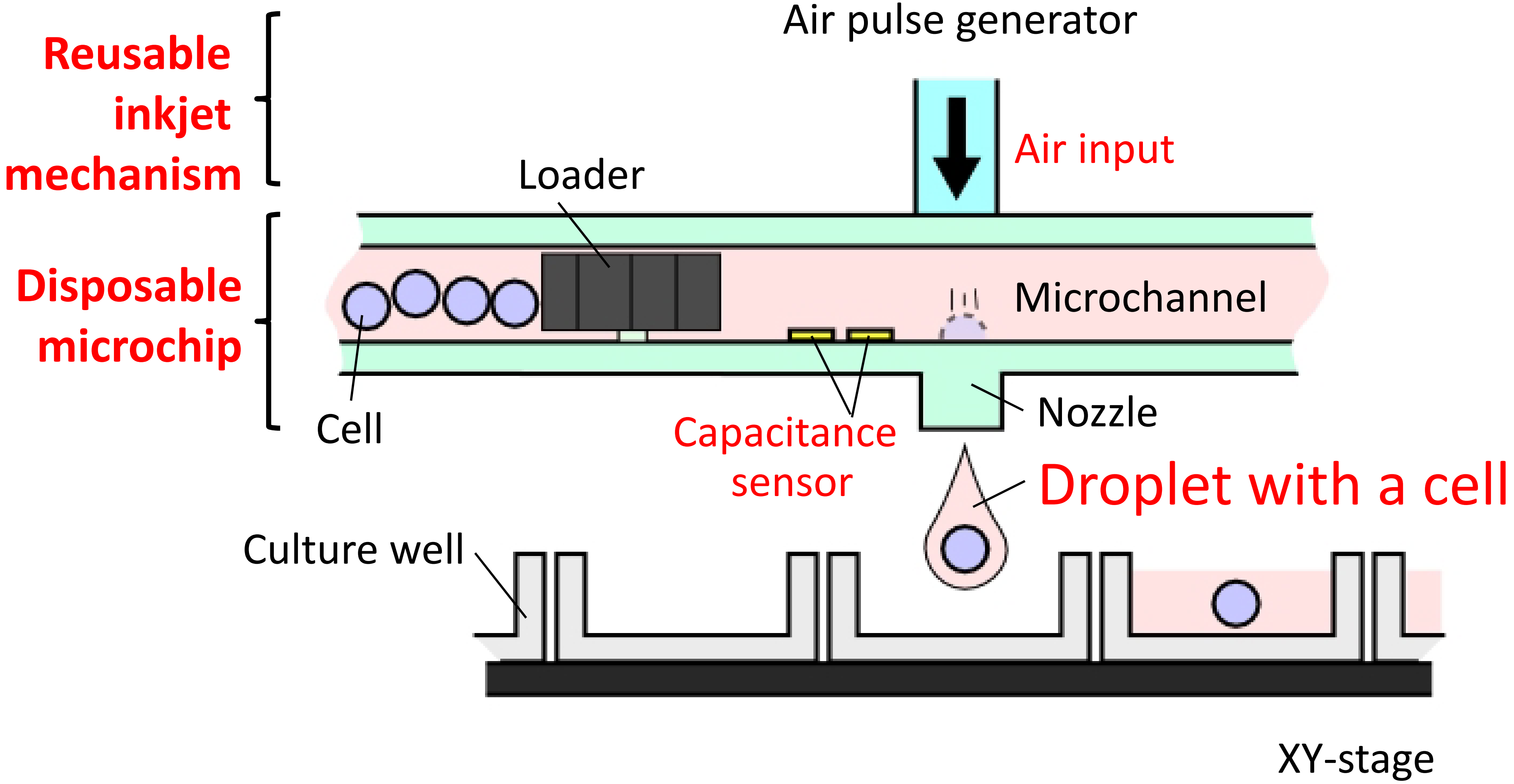

Inkjet Mechanism with Disposable Structure
（JPN Patent: 2009-91542）

Capacitance Sensor

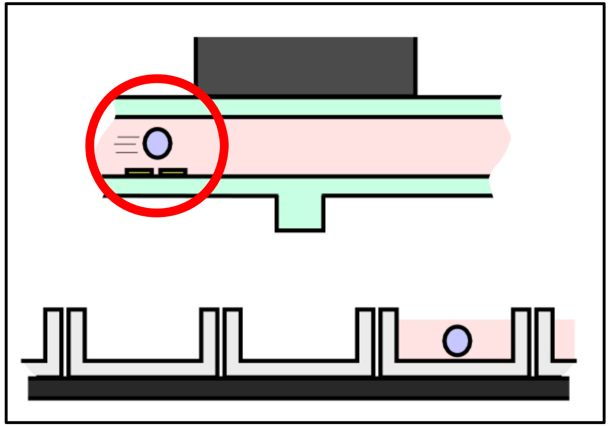

FEM analysis:

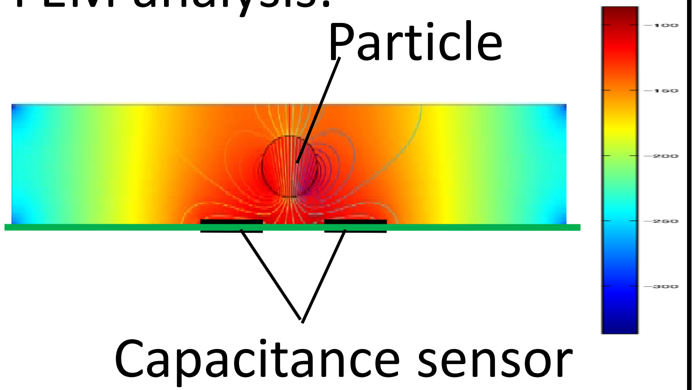

Condition: $V_0 = V_{in} \sin(2\pi f t)$[V]

V_{in}=0.1[V]

f = 100 [kHz]

t = 0～1e-5 (1e-8)

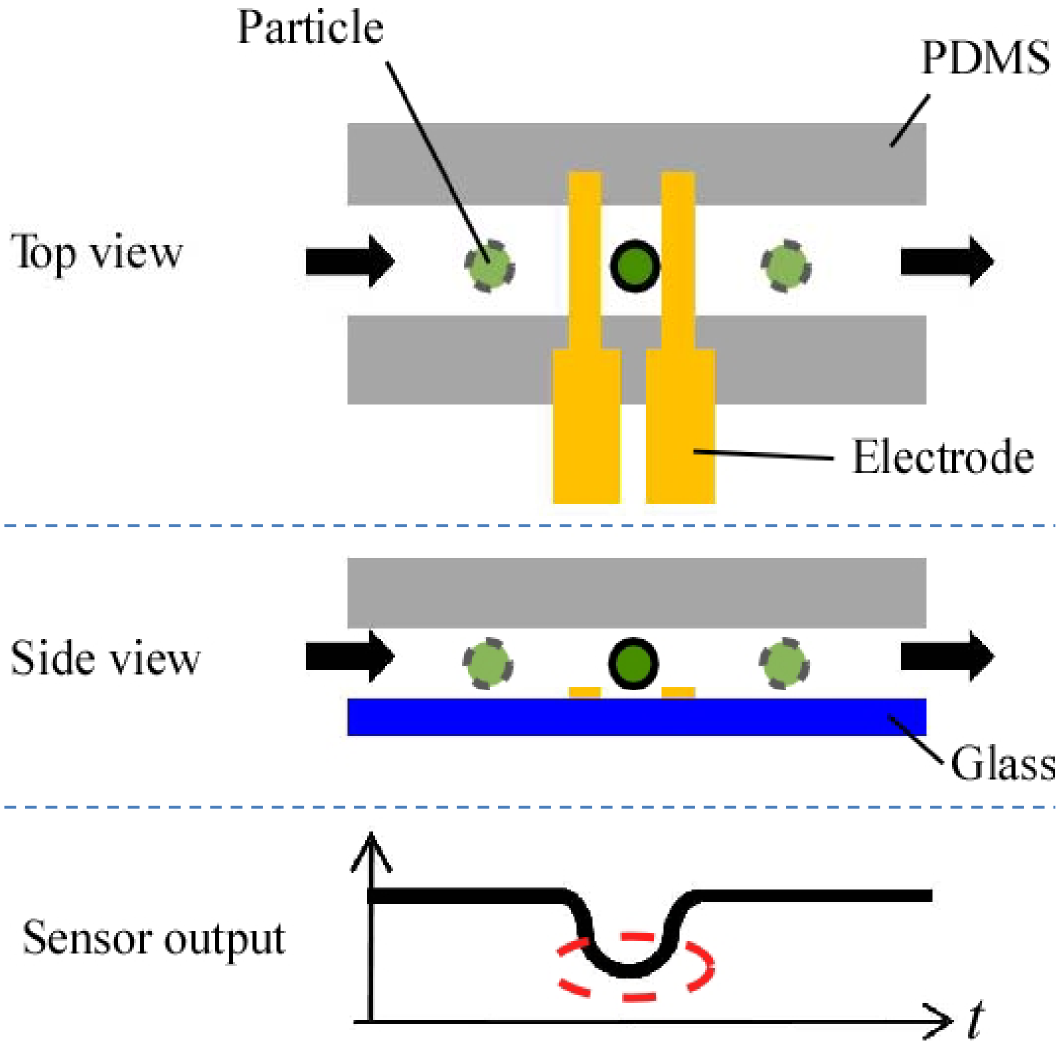

$$V = I\sqrt{R^2 + \left(\frac{1}{\omega C}\right)^2}, \quad C = \frac{Q}{2V_0} = \frac{2\varepsilon_r \varepsilon_0 I}{\pi} \ln\left[\left(1 + \frac{w}{a}\right) + \sqrt{\left(1 + \frac{w}{a}\right)^2 - 1}\right]$$

Fabrication Process

1. Nozzle

1. Drilling

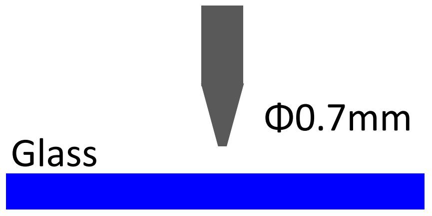

2. Nozzle assemble

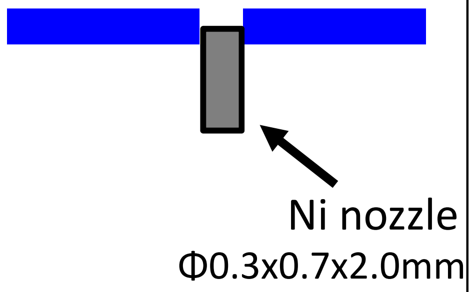

2. Electrode

1.Supatter(Cr/Au)
& Resist patterning

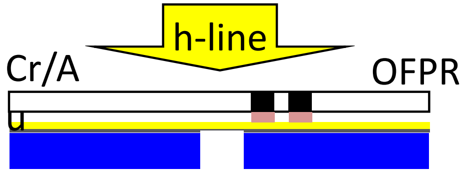

2. Au wet etching

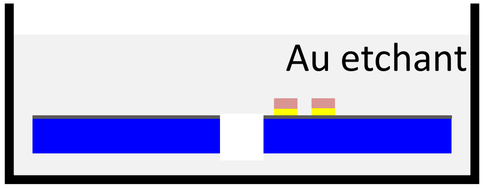

3.Cr wet etching

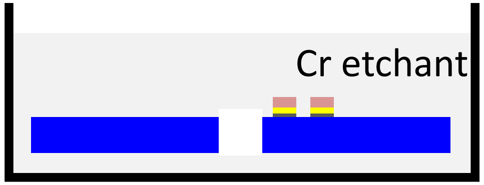

3. Micro-channel

1.PDMS molding

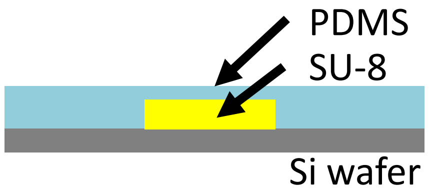

2.Assmbly (Plasma)

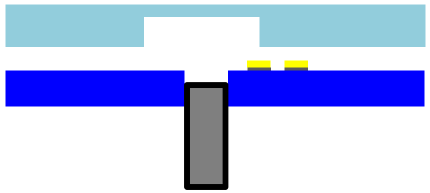

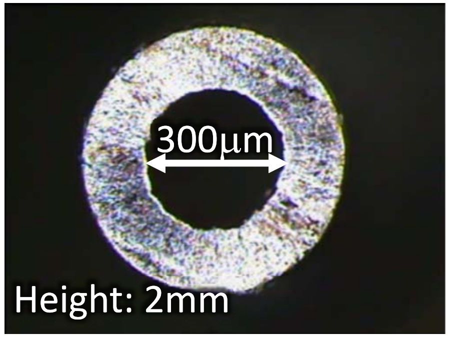

Height: 2mm

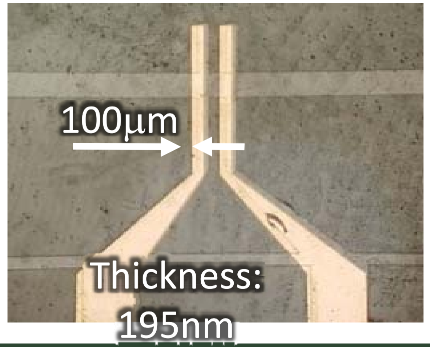

Thickness: 195nm

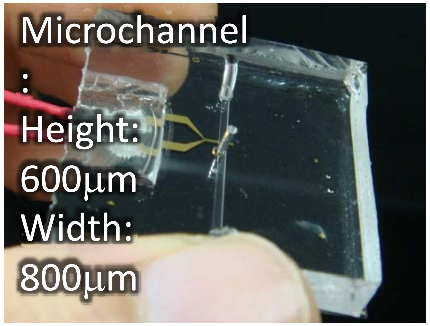

Microchannel
:
Height: 600μm
Width: 800μm

Fabricated Microchip

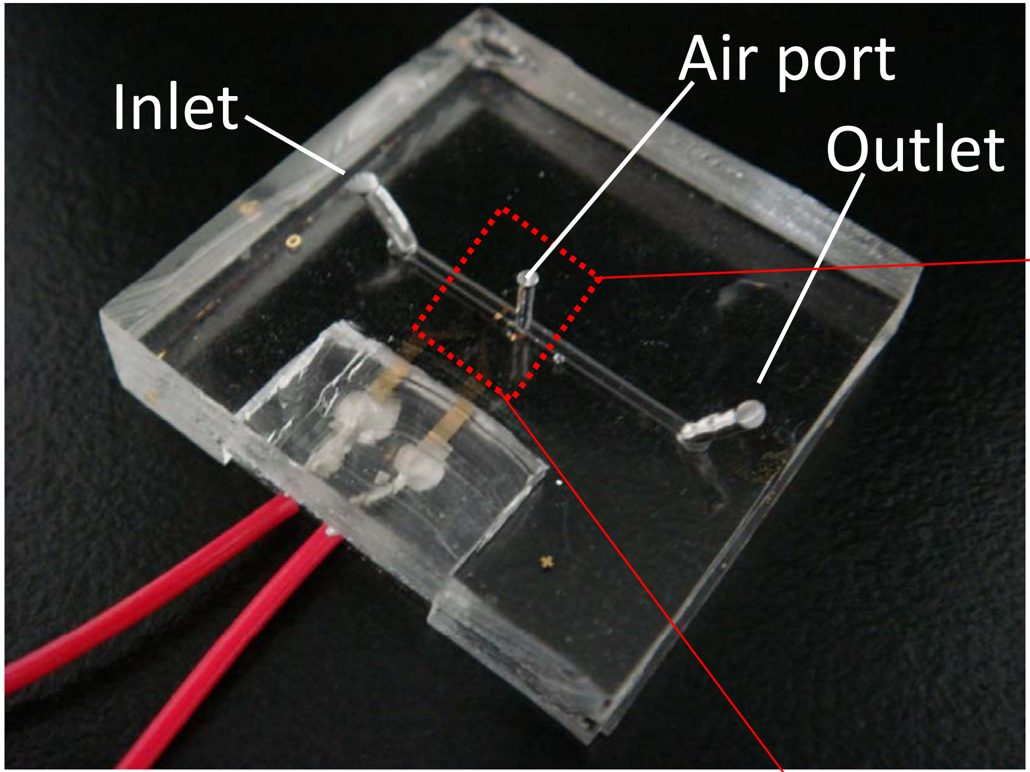

Disposable microchip
(30x30 mm)

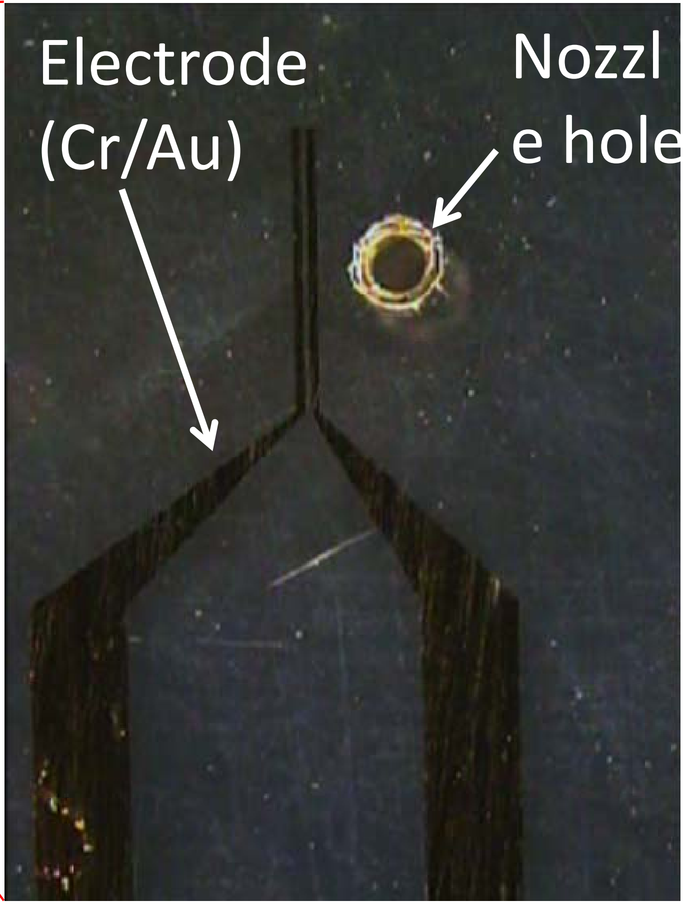

Experimental Setup

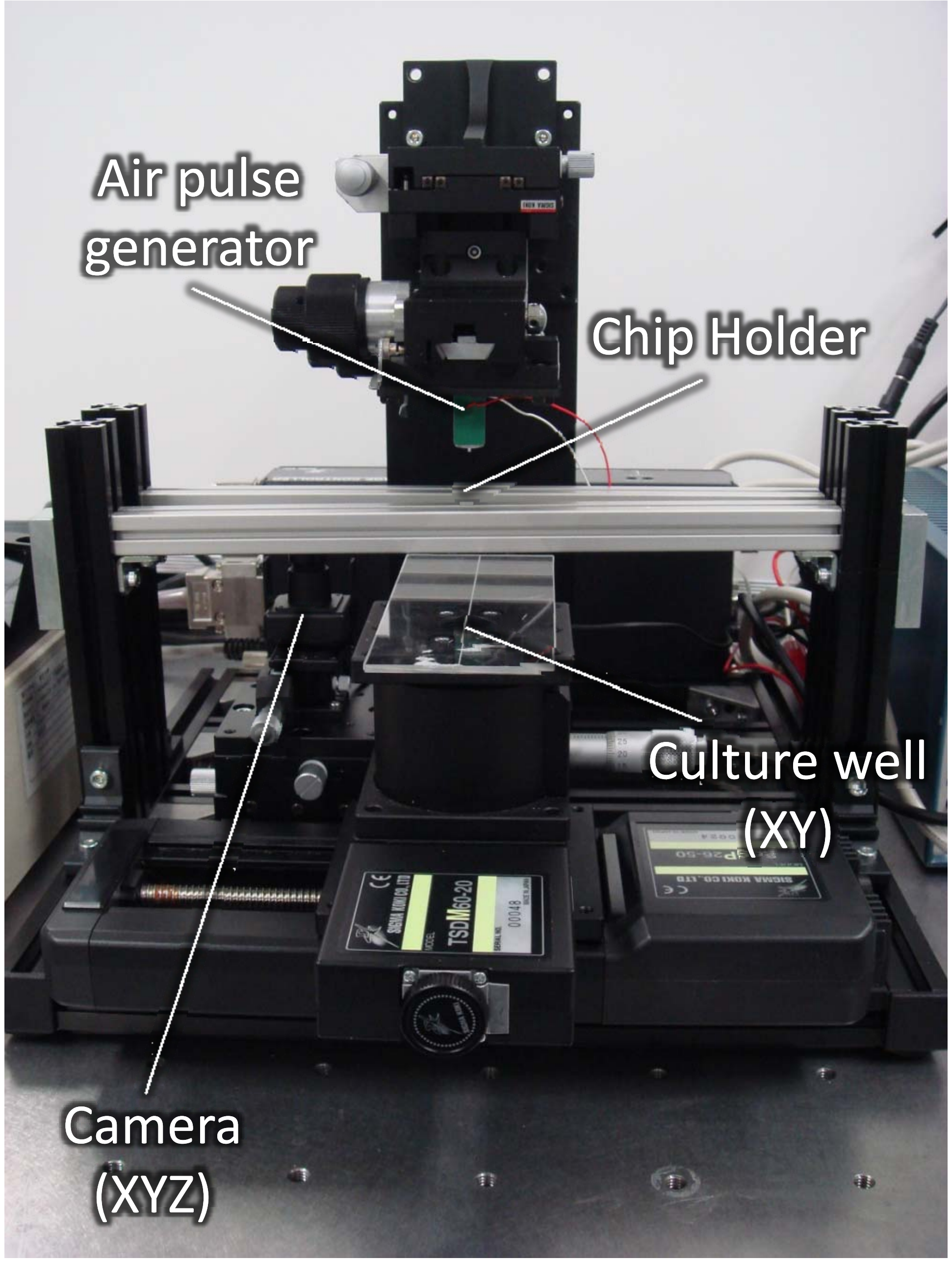

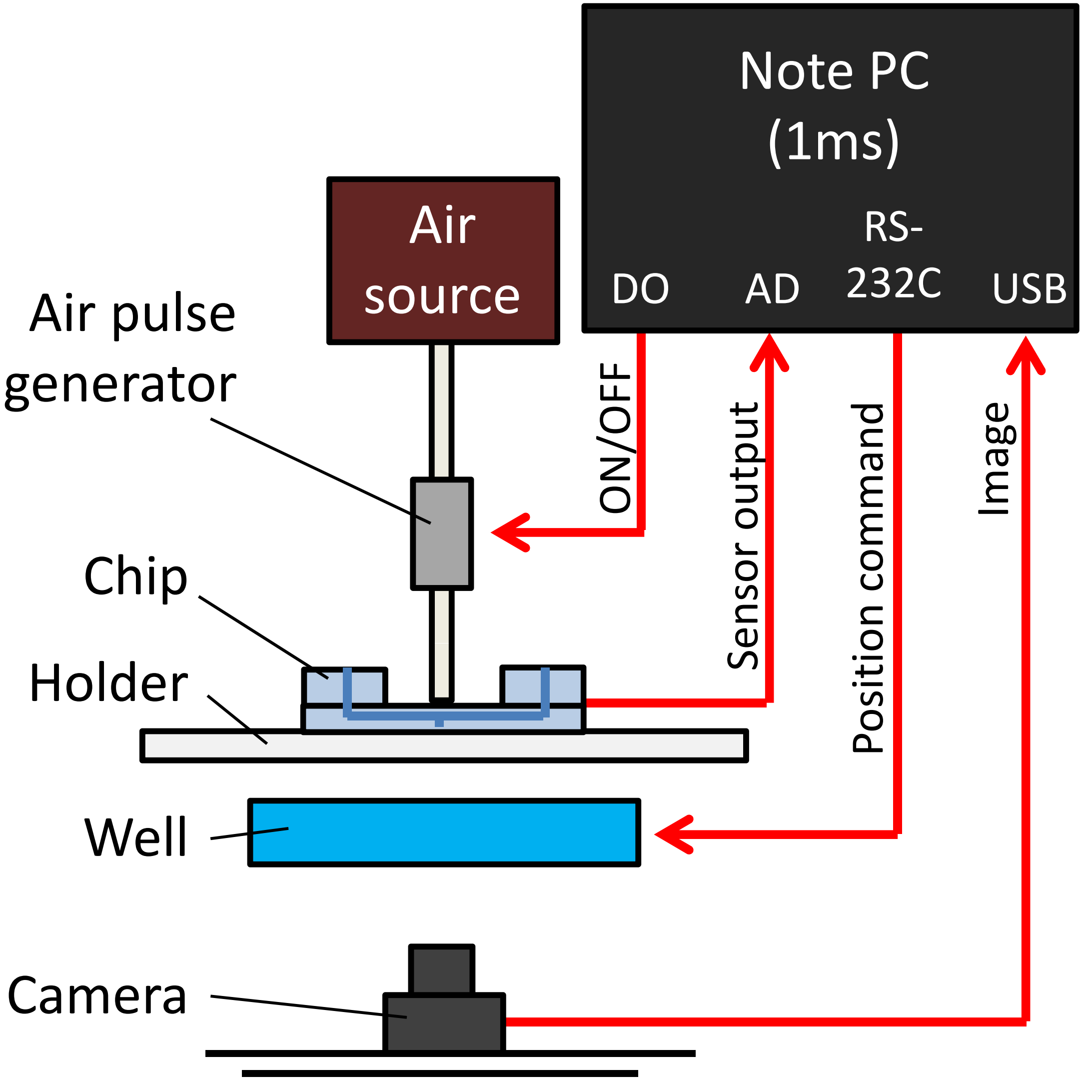

Droplet generation and Dispensing

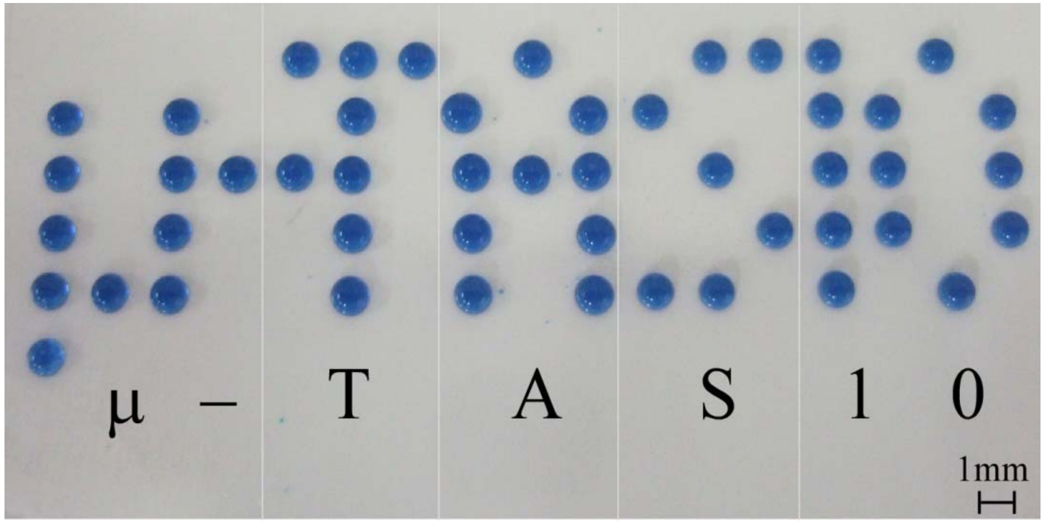

Droplet size：1mm
Droplet volume: approx. 0.4µl

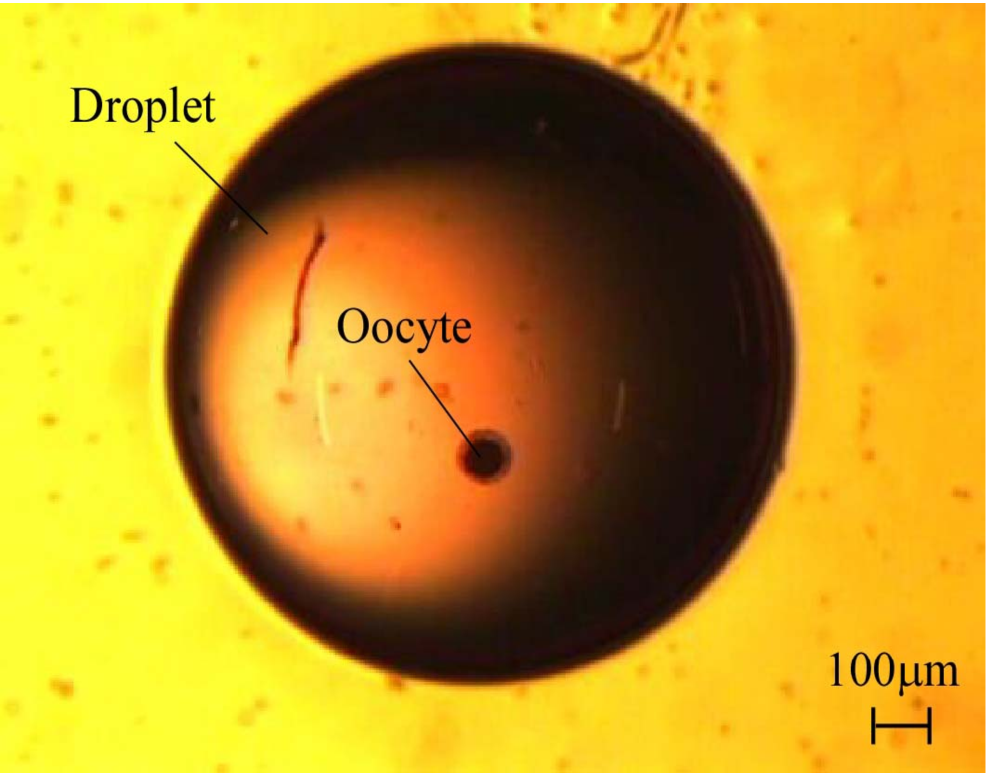

We succeeded in the single swine oocyte dispensing.

References

1. K. Narumi, D. Azuma, and F. Arai:
Fabrication of Articulated Microarm for Endoscopy by Stacked Microassembly Process (STAMP),
Journal of Robotics and Mechatronics, Vol. 22, No. 3, pp. 412-418, 2009.

2. T. Kawahara, T. Matsumoto, N. Muramatsu, T. Osada, N. Sakamoto, and F. Arai:
Development of a Decoupling Wire Driven Exoskeletal Microarm for Endoscopic Submucosal Dissection,
Proc. of the 3rd IEEE/RAS-EMBS Int. Conf. on Biomedical Robotics and Biomechatronics, pp. 849-854, 2010.

3. K. Narumi, A. Asakura, T. Fukuda, and F. Arai :
Design, Fabrication and Characterization of Compact Force Sensor using AT-cut Quartz Crystal Resonators,
Journal of Robotics and Mechatronics, Vol. 21, No. 2, pp. 260–266, 2009.

4. K. Narumi, T. Fukuda, and F. Arai:
Design and Characterization of Load Sensor with AT-Cut QCR for Miniaturization and Resolution Improvement ,
Journal of Robotics and Mechatronics, Vol. 22, No. 3, pp. 286-292, 2010.

5. N. Inomata, Y. Yamanishi, and F. Arai:
Manipulation and Observation of Carbon Nanotubes in Water Under an Optical Microscope Using a Microfluidic Chip,
IEEE Transactions on Nanotechnology, Vol. 8, Issue. 4, pp. 463-468, 2009

6. T. Mizunuma, Y. Yamanishi, S. Sakuma, H. Maruyama, and F. Arai:
Disposable Inkjet Mechanism for Microdroplet Dispensing,
Journal of Robotics and Mechatronics, Vol. 22, No. 3, pp. 341-347, 2010.

7. T. Kawahara, T. Mizunuma, H. Uvet, M. Hagiwara, Y. Yamanishi, and F. Arai:
Development of On-Chip Automatic Cell Sensing and Ejection System,
Proc. of the 14th Int. Conf. on Miniaturized Systems for Chemistry and Life Sciences, pp. 1781-1783, 2010.